

Communication-Efficient Federated Low-Rank Update Algorithm and its Connection to Implicit Regularization

Haemin Park & Diego Klabjan
Department of Industrial Engineering & Management Sciences
Northwestern University
Evanston, IL, USA
{haemin.park1,d-klabjan}@northwestern.edu

Abstract

Federated Learning (FL) faces significant challenges related to communication efficiency and heterogeneity. To address these issues, we explore the potential of using low-rank updates. Our theoretical analysis reveals that client’s loss exhibits a higher rank structure (gradients span higher rank subspace of Hessian) compared to the server’s loss. Based on this insight, we hypothesize that constraining client-side optimization to a low-rank subspace could provide an implicit regularization effect. Consequently, we propose FedLoRU, a general low-rank update framework for federated learning. Our framework enforces low-rank client-side updates and accumulates these updates to form a higher-rank model. Additionally, variants of FedLoRU can adapt to environments with statistical and model heterogeneity by employing multiple or hierarchical low-rank updates. Experimental results demonstrate that FedLoRU performs comparably to full-rank algorithms and exhibits robustness to heterogeneous and large numbers of clients.

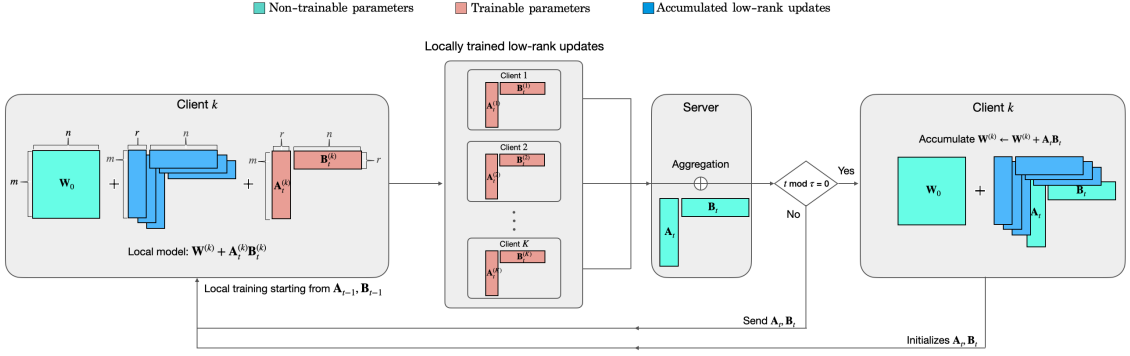
1 Introduction

Federated learning (McMahan et al., 2017) is a collaborative learning framework designed to enhance privacy preservation in machine learning applications. This approach has gained importance due to rising concerns over data privacy, as it allows multiple participants to train a model collectively without sharing raw data.

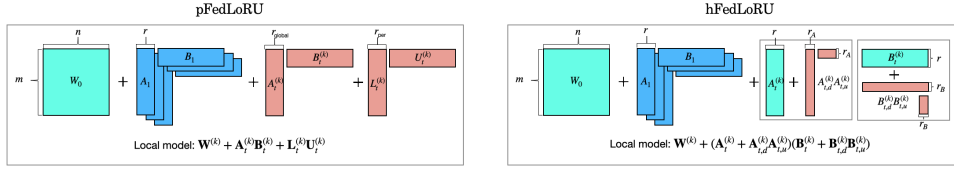
While federated learning offers privacy benefits, it trades off some performance compared to centralized learning. Two primary factors contributing to this trade-off are communication overhead and heterogeneity. Despite improvements in computation and memory capacities, communication speeds have only slightly improved, making communication overhead a major factor in slowing down federated learning (Zheng et al., 2020). Additionally, various forms of heterogeneity—statistical, system, and device—further complicate FL (Kairouz et al., 2021; Ye et al., 2023). These issues are especially pronounced with a large number of clients, where frequent, less impactful updates slow down training and reduce performance.

Addressing these challenges is becoming increasingly critical for training large language models (LLMs) in a federated learning framework. By low rank herein we refer to gradients spanning a low rank subspace of Hessian at any weights or the weight matrix being of the form \mathbf{AB} where the number of columns of \mathbf{A} is low. Utilizing private datasets on edge devices for LLM training is promising due to the limited availability of public data (Ye et al., 2024). However, this approach presents significant issues, notably in terms of communication overhead, as edge devices possess heterogeneous resources and data. Additionally, the need for effective regularization across clients is required. Consequently, the development of algorithms to tackle these challenges is an essential problem to bridge the gap between practical and conceptual federated learning applications.

There has been substantial research focusing on the low-rank characteristics in centralized learning. Utilizing low-rank factorized update models such as LoRA (Hu et al., 2021), DyLoRA (Valipour et al., 2022), and QLoRA (Dettmers et al., 2024) can significantly reduce the number of trainable parameters, which helps to conserve memory and computational resources. Further observations (Huh et al., 2021; Ji and Telgarsky, 2018) indicate that over-parameterized models tend to find low-rank solutions, which provide implicit regularization effects.



(a) Flow-chart of FedLoRU algorithm



(b) Low-rank factorization methods in pFedLoRU and mFedLoRU

Figure 1: Figure 1(a) provides a flowchart representing the FedLoRU algorithm. In this algorithm, the model training is conducted solely using rank- r matrices, with communication between the server and clients being confined to these matrices. Clients incrementally add low-rank update matrices to their local base model $\mathbf{W}^{(k)}$ every τ rounds, resulting in a higher-rank model. Figure 1(b) depicts the utilization of low-rank factorization within the pFedLoRU and mFedLoRU algorithms. For clarity, the equations assume all α parameters are set to 1.

However, the rank properties of the loss landscape in federated learning remain under-explored. We first analyze the difference in the stable rank—defined as the squared ratio of the Frobenius norm to the spectral norm—between client Hessians and the server Hessian of any weights, discovering that client exhibits a higher rank structure. Based on this theoretical insight, we hypothesize that the higher rank structure of client’s loss contributes to increased client discrepancy and that restricting client-side updates could provide an implicit regularization effect across clients. This leads us to the research question:

Can we use low-rank updates to achieve both communication overhead reduction and regularization effects across clients?

We propose the Federated Low-Rank Updates (FedLoRU) algorithm, which addresses communication overhead and the challenges posed by a large number of clients by employing client-side low-rank updates and server-side accumulation of low-rank updates. FedLoRU factorizes client-side update matrices \mathbf{A} and \mathbf{B} and applies iterative optimization to these low-rank factorized matrices. Clients and the server share the factorized matrices, which the server then aggregates. Matrices \mathbf{A} and \mathbf{B} are communicated between the clients and server, rather than the much larger matrix \mathbf{AB} . To make the model’s weight rank high, the server successively accumulates low-rank matrices. We also generalize the low-rank update strategy within federated learning for various heterogeneous settings.

Our comprehensive approach underscores the potential of low-rank updates not only to enhance communication efficiency but also to impose implicit regularization and harmonize the optimization process across heterogeneous federated learning settings. Our contributions can be summarized as follows. 1) We propose FedLoRU, the first algorithm using successive low-rank updates for both pre-training and fine-tuning in federated learning, and introduce variants of FedLoRU for personalization and model heterogeneity settings; 2) We investigate the rank properties of client and server losses, analytically showing that under stochastic sampling, the rank of the Hessian of the loss function increases with smaller sample sizes; 3) We provide empirical evidence of the higher rank structure of client losses and demonstrate that restricting the rank of local updates aids in implicit regularization; 4) On average, FedLoRU improves state-of-the-art communication-efficient federated learning algorithms on a variety of datasets, including LLM fine-tuning, and exhibits superior performance as the number of clients increases.

2 Related work

Communication-Efficient Federated Learning Extensive research has been conducted to address the communication challenges in federated learning (Shahid et al., 2021). FedPAQ (Reisizadeh et al., 2020) and AdaQuantFL (Jhunjhunwala et al., 2021) employ quantization techniques that decrease the precision of weights and activations in neural networks. Besides, Fed-Dropout (Caldas et al., 2018) and FedMP (Jiang et al., 2023) utilize pruning to eliminate less important neurons or connections within models. Since quantization and sparsification techniques do not alter the fundamental network architecture and can be universally applied across any models, they are perceived as additional steps aimed at reducing communication overhead.

In contrast to these methods, model compression techniques in federated learning alter the model structure itself by transforming the original model into a smaller model update before communication, then restoring it before local training or aggregation. FedDLR (Qiao et al., 2021) employs low-rank approximation to compress the model during both server-to-client and client-to-server communications, reverting to the full-rank model during local training. On the other hand, FedHM (Yao et al., 2021) compresses the model solely during server-to-client communication, where clients train factorized low-rank models without reverting them and the server restores the local models before aggregation. While both FedDLR and FedHM effectively reduce communication overheads, their server-side compression approaches can lead to performance degradation. To mitigate potential information loss during server-side compression, we focus on client-side factorization, avoiding compression processes.

Low-rank nature of centralized and federated learning Despite the over-parameterization of current deep learning models, numerous studies (Gur-Ari et al., 2018; Li et al., 2018; Sagun et al., 2016) assert that the training process in deep learning inherently possesses a low-rank nature. Low-Rank Adaptation (LoRA, Hu et al. (2021)) is a representative algorithm that leverages this low-rank characteristic, particularly for fine-tuning tasks. However, effectively utilizing the low-rank structure during the pre-training phase remains challenging. This difficulty is elucidated by some papers (Yu and Wu, 2023; Zhao et al., 2024), which attribute the issue to the weights not exhibiting a low-rank.

Existing research in federated learning has attempted to exploit the low-rank nature observed in centralized learning. LBG (Azam et al., 2021) and FedLRGD (Jadbabaie et al., 2023) approximate gradients by utilizing old or sampled gradients under the assumption that gradients live in a low-rank subspace. Nonetheless, there is a noticeable gap in their assumption and analysis regarding the rank characteristics specific to federated learning. In the context of federated learning, there is a complex loss landscape involving multiple client-side and a single server-side optimization, and leveraging a low-rank structure needs to consider their respective rank structures. To our knowledge, no prior work has examined the rank structure in federated learning contexts without making very stringent assumptions. Our study is pioneering in addressing this gap, using analytical results and insights to develop a novel algorithm.

Low-Rank Adaptation The fundamental concept of LoRA involves freezing the pre-trained weights and adapting them to new tasks by introducing and optimizing an update through a two-layer low-rank decomposition. This is represented mathematically as $\mathbf{W} = \mathbf{W}_0 + \mathbf{A}\mathbf{B}$ where $\mathbf{W} \in \mathbb{R}^{m \times n}$, $\mathbf{A} \in \mathbb{R}^{m \times r}$, $\mathbf{B} \in \mathbb{R}^{r \times n}$, $r \ll m, n$. By constraining the update matrix to a low-rank factorization, the number of parameters in the update matrix is reduced. However, this method demonstrates suboptimal performance during pre-training because the trained weight matrix does not exhibit a low-rank structure. To address this, ReLoRA (Lialin et al., 2023) seeks to achieve a higher-rank model by accumulating multiple low-rank updates, expressed as $\mathbf{W} = \mathbf{W}_0 + \sum_{i=1}^M \mathbf{A}_i \mathbf{B}_i$ where $\mathbf{A}_i \in \mathbb{R}^{m \times r}$, $\mathbf{B}_i \in \mathbb{R}^{r \times n}$.

Low-Rank Adaptation in Federated Learning Recent studies have studied the application of LoRA within federated learning frameworks. Notable algorithms, such as FedLoRA (Wu et al., 2024; Yi et al., 2023), FFALoRA (Sun et al., 2024), and Hyperflora (Lu et al., 2024), employ LoRA adapters to facilitate personalization. These methods apply low-rank adaptation to a pre-trained model during the local personalization training phase. On the other hand, other works such as Kuo et al. (2024) and Cho et al. (2023) apply LoRA for fine-tuning within federated learning environments.

These approaches use only one low-rank matrices that restricts the model to lie in low-rank subspace, on the other hand, our work utilizes multiple accumulated layers of low-rank matrices allowing the model to achieve higher rank. Specifically, we extend the concept of LoRA by incorporating client-side

low-rank updates and server-side accumulation, aiming to address the low-rank limitation of LoRA as well as the challenges posed by communication and client-server rank disparity. We also generalize the low-rank strategy within federated learning for both pre-training and fine-tuning, and for heterogeneous environments.

3 Low-rank updates in federated learning

In centralized learning, neural network losses exhibit a low-rank structure, indicating that the gradient lies within the subspace spanned by the k eigenvectors of the Hessian (Gur-Ari et al., 2018) during training. While efforts have been made to utilize this low-rank structure to enhance federated learning algorithms, there is a lack of studies analyzing the rank structure of federated learning. In federated learning, the clients and server have distinct losses, resulting in different rank structures. Understanding these differing rank structures of client and server losses is crucial for developing low-rank-inspired algorithms tailored for federated learning.

In this section, we conduct a theoretical analysis of the rank structure of federated learning, with a particular emphasis on comparing the rank of client and server Hessians. Drawing from this theoretical analysis, we propose a novel federated learning algorithm FedLoRU designed to address communication efficiency and performance degradation issues associated with a large number of clients. Additionally, we introduce an algorithm that modifies FedLoRU to address challenges related to model and statistical heterogeneity in federated learning.

3.1 Higher rank nature of clients in federated learning

Notation and problem setup Suppose $\psi(\mathbf{x}, \mathbf{y})$ is a data generating distribution for an input-output pair $(\mathbf{x}, \mathbf{y}) \in \mathbb{R}^{d_x} \times \mathbb{R}^{d_y}$. We consider the problem of finding a prediction function $h^R(\cdot; \cdot) : \mathbb{R}^{d_x} \times \mathbb{R}^R \rightarrow \mathbb{R}^{d_y}$ parameterized by a R -dim weight vector $\omega^R \in \mathbb{R}^R$. Given a loss function $\ell(\cdot, \cdot) : \mathbb{R}^{d_y} \times \mathbb{R}^{d_y} \rightarrow \mathbb{R}$, the true or population risk is defined as the loss over the data-generating distribution $\psi(\mathbf{x}, \mathbf{y})$

$$\mathcal{L}_{\text{true}}(h^R, \omega^R) = \int \ell(h^R(\mathbf{x}; \omega^R), \mathbf{y}) d\psi(\mathbf{x}, \mathbf{y}). \quad (1)$$

The corresponding true Hessian is $\mathbf{H}_{\text{true}}(h^R, \omega^R) = \nabla^2 \mathcal{L}_{\text{true}}(h^R, \omega^R)$. If $\mathcal{D}_N = \{(\mathbf{x}_1, \mathbf{y}_1), \dots, (\mathbf{x}_N, \mathbf{y}_N)\}$ is a dataset generated from the distribution ψ , then the loss and Hessian corresponding to the dataset \mathcal{D}_N are given by:

$$f_N(h^R, \omega^R) = \sum_{(x,y) \in \mathcal{D}_N} \frac{1}{N} \ell(h^R(x; \omega^R), y), \quad \mathbf{H}_N(h^R, \omega^R) = \sum_{(x,y) \in \mathcal{D}_N} \frac{1}{N} \frac{\partial^2}{\partial (\omega^R)^2} \ell(h^R(x; \omega^R), y). \quad (2)$$

We consider random selection of M samples without replacement from \mathcal{D}_N to form a sub-dataset $\mathcal{D}_M \subseteq \mathcal{D}_N$. Let $f_M(h^R, \omega^R)$ and $\mathbf{H}_M(h^R, \omega^R)$ denote the loss and Hessian for the sub-dataset \mathcal{D}_M . For simplicity, we omit the explicit dependency on h^R and ω^R when contextually clear. In federated learning, f_N can be considered as the loss that the server optimizes, while f_M represents the loss of a local client assuming the homogeneous setting.

For non-zero real numbers $\theta_1, \dots, \theta_k$, define $\Omega^R(\theta_1, \dots, \theta_k)$ as the family of pairs (h^R, ω^R) , where h^R is an R -dimensional prediction function and ω^R is a weight vector, such that the true Hessian has eigenvalues $\theta_1, \dots, \theta_k$. Specifically, $\Omega^R(\theta_1, \dots, \theta_k) = \{(h^R, \omega^R) : \mathbf{H}_{\text{true}}(h^R, \omega^R) \text{ has eigenvalues } \theta_1, \dots, \theta_k\}$. Let $\Omega(\theta_1, \dots, \theta_k) = \bigcup_R \Omega^R(\theta_1, \dots, \theta_k)$, representing the union of $\Omega^R(\theta_1, \dots, \theta_k)$ over all dimensions R . We aim to show that the difference in stable rank between the Hessians of a server and a client eventually becomes positive as dimension R approaches infinity within the space of $\Omega(\theta_1, \dots, \theta_k)$.

In fact, the set of all possible pairs (h^R, ω^R) is represented by the union over all dimensions R , integers $k \leq R$, and non-zero real values $\theta_1, \dots, \theta_k$ as follows:

$$\{(h^R, \omega^R) : \text{dimension } R < \infty\} = \bigcup_{R=1}^{\infty} \bigcup_{k=1}^R \bigcup_{(\theta_1, \dots, \theta_k) \in \mathbb{R}^k} \Omega^R(\theta_1, \dots, \theta_k).$$

Thus, for any given pair (h^R, ω^R) , there exist $\theta_1, \dots, \theta_k$ such that $(h^R, \omega^R) \in \Omega^R(\theta_1, \dots, \theta_k)$. According to the following proposition, the proof of which is provided in Appendix A.1, either the set $\Omega(\theta_1, \dots, \theta_k)$ is empty or there exist infinitely many values of R for which $\Omega^R(\theta_1, \dots, \theta_k) \neq \emptyset$.

Proposition 3.1. *Let $\theta_1, \dots, \theta_k$ be fixed non-zero real numbers, and suppose there exists $\tilde{R} > k$ such that $\Omega^{\tilde{R}}(\theta_1, \dots, \theta_k)$ is non-empty. Then there are infinitely many R such that $\Omega^R(\theta_1, \dots, \theta_k)$ is non-empty. In particular, $\Omega^R(\theta_1, \dots, \theta_k)$ is non-empty for all $R \geq \tilde{R}$.*

Comparing the stable rank of the client and server Hessians Now, we will focus on comparing the stable rank of the client and server Hessians. For given $p, q \in \mathbb{N}$, let $\theta_1 > \dots > \theta_p > 0 > \theta_{p+1} > \dots > \theta_{p+q}$ be deterministic non-zero real numbers, and let $(h^R, \omega^R) \in \Omega(\theta_1, \dots, \theta_{p+q})$ for some R . To compare the stable rank of Hessians for two datasets \mathcal{D}_N and \mathcal{D}_M , we consider the additive perturbed model of the true Hessian as described by [Baskerville et al. \(2022\)](#):

$$\mathbf{H}_N(h^R, \omega^R) = \mathbf{H}_{\text{true}}(h^R, \omega^R) + \epsilon^R(N) \quad (3)$$

$$\mathbf{H}_M(h^R, \omega^R) = \mathbf{H}_{\text{true}}(h^R, \omega^R) + \epsilon^R(M). \quad (4)$$

Here, $\epsilon^R(N), \epsilon^R(M) \in \mathbb{R}^{R \times R}$ are defined as random error matrices associated with each Hessian. These matrices are assumed to be scaled according to $\epsilon^R(N) = s(N)X^R$, where $X^R \in \mathbb{R}^{R \times R}$ is a random real symmetric matrix and $s : \mathbb{N} \rightarrow (0, 1)$ is a decreasing function.

Another study ([Granzoli et al., 2022](#)) employs the model $\mathbf{H}_M(h^R, \omega^R) = \mathbf{H}_N(h^R, \omega^R) + \epsilon^R$, implying a dependency structure between \mathbf{H}_M and \mathbf{H}_N . However, their analysis assumes independence between these matrices, which is problematic given the underlying model and practical considerations. In contrast, we address this issue by introducing two decoupled additive perturbed models. Additionally, while [Granzoli et al. \(2022\)](#) investigates outlier eigenvalues, our focus is on the difference in the rank of the Hessians.

We seek to determine the limiting eigenvalues of the Hessians $\mathbf{H}_N(h^R, \omega^R)$ and $\mathbf{H}_M(h^R, \omega^R)$ in relation to the eigenvalues of $\mathbf{H}_{\text{true}}(h^R, \omega^R)$. Since $(h^R, \omega^R) \in \Omega^R(\theta_1, \dots, \theta_{p+q})$, the eigenvalues of $\mathbf{H}_{\text{true}}(h^R, \omega^R)$ are $\theta_1, \dots, \theta_{p+q}$. Next, we need to make some assumptions about the random error matrix X^R . Assume X^R is a random real symmetric matrix with eigenvalues $\lambda_1(X^R), \dots, \lambda_R(X^R)$ and a limiting spectral density μ , such that $\frac{1}{R} \sum_{i=1}^R \delta(\lambda - \lambda_i(X^R)) \rightarrow \mu(\lambda)$, with convergence in the weak almost sure sense. Examples of matrices exhibiting a well-defined limiting spectral density include Wigner matrices, Wishart matrices, and Gaussian ensembles. We assume μ is a compactly supported probability measure on $[l_\mu, r_\mu]$ which admits a smooth density with respect to the Lebesgue measure and the eigenvectors of X^R obey quantum unique ergodicity (QUE). For more detail about the QUE condition, we refer to [Baskerville et al. \(2022\)](#). We can now find the limiting eigenvalues of \mathbf{H}_N and \mathbf{H}_M .

Proposition 3.2 (Limiting eigenvalues of \mathbf{H}_N (modified from [Baskerville et al. \(2022\)](#))). *Let R be any integer such that $R \geq \bar{R}$ where \bar{R} is the smallest integer such that $\Omega^{\bar{R}}(\theta_1, \dots, \theta_{p+q})$ is non-empty. For any pair $(h^R, \omega^R) \in \Omega^R(\theta_1, \dots, \theta_{p+q})$, consider the Hessian additive error model given by $\mathbf{H}_N(h^R, \omega^R) = \mathbf{H}_{\text{true}}(h^R, \omega^R) + \epsilon^R(N)$. If $\lambda_i(\mathbf{H}_N(h^R, \omega^R))$ denotes the i -th eigenvalue of $\mathbf{H}_N(h^R, \omega^R)$, then for $i = 1, \dots, p$, the following holds:*

$$\lambda_i(\mathbf{H}_N(h^R, \omega^R)) \rightarrow \begin{cases} g_N^{-1}(\theta_i) & \text{if } g_N^{-1}(\theta_i) > U_N \\ U_N & \text{otherwise} \end{cases} \quad (5)$$

as $R \rightarrow \infty$, while for each fixed $i > p$, $\lambda_i(\mathbf{H}_N(h^R, \omega^R))$ that converges to a limit in $\mathbb{R} \setminus [0, U_N]$ converges to U_N , i.e., $\lambda_i(\mathbf{H}_N(h^R, \omega^R)) \rightarrow U_N$. Similarly, for $i = 0, \dots, q-1$, we have

$$\lambda_{R-i}(\mathbf{H}_N(h^R, \omega^R)) \rightarrow \begin{cases} g_N^{-1}(\theta_{p+q-i}) & \text{if } g_N^{-1}(\theta_{p+q-i}) < L_N \\ L_N & \text{otherwise} \end{cases} \quad (6)$$

while for each fixed $i \geq q$, $\lambda_{R-i}(\mathbf{H}_N(h^R, \omega^R))$ that converges to a limit in $\mathbb{R} \setminus [L_N, 0]$ converges to L_N , i.e., $\lambda_{R-i}(\mathbf{H}_N(h^R, \omega^R)) \rightarrow L_N$. Here,

$$g_N^{-1}(\theta) = \theta + s(N)\mathcal{R}_\mu(s(N)\theta^{-1}) \quad (7)$$

and U_N and L_N are lower and upper bounds of the limiting distribution μ_N of $\epsilon^R(N)$.

Convergence in Proposition 3.2 is weak almost sure convergence and $\mathcal{R}_\mu(\omega)$, known as the \mathcal{R} -transform, is defined by $\mathcal{R}_\mu(\omega) = S_\mu^{-1}(\omega) - \frac{1}{\omega}$ where $S_\mu(\omega)$ is the Stieltjes transform. Compared to [Baskerville et al. \(2022\)](#), which focuses solely on outlier eigenvalues, we extend the analysis to bulk eigenvalues and adopt a

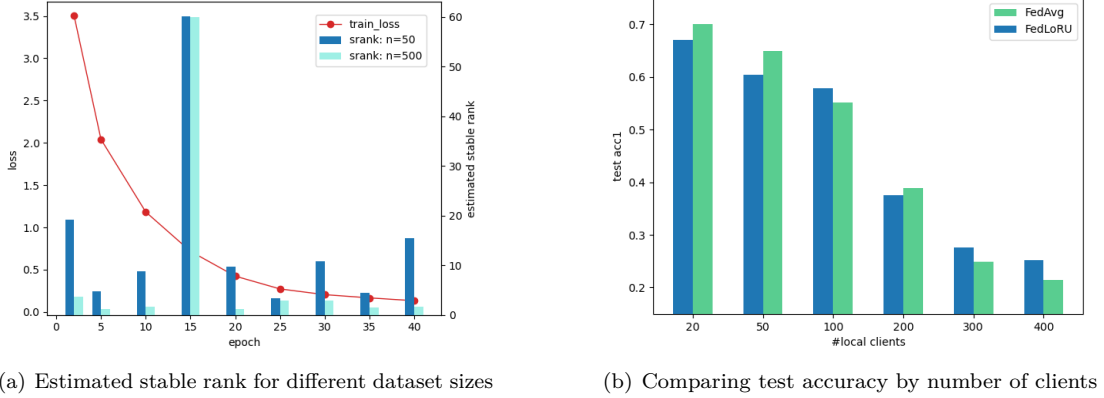


Figure 2: Figure 2(a) presents a comparison of the estimated stable rank of the Hessian for dataset sizes of 50 and 500. The estimated spectral density was computed using the pyhessian (Yao et al., 2020) library, and the stable rank was subsequently derived from these estimates. The stable rank of the Hessian for the dataset size of 50 consistently exceeds that of the dataset size of 500. Figure 2(b) illustrates the test accuracy of FedAvg and FedLoRU across varying numbers of clients. Notably, as the number of clients increases, FedLoRU demonstrates better accuracy compared to FedAvg.

simpler form of μ . Within the proposition, the i -th largest or smallest limiting eigenvalues of \mathbf{H}_N are determined by the values of $g^{-1}(\theta_i)$. If $g^{-1}(\theta_i)$ falls within the support of the limiting distribution μ_N , the corresponding limiting eigenvalues converge to the bounds. If $g^{-1}(\theta_i)$ does not lie within this support, it converges to $g^{-1}(\theta_i)$ itself; these eigenvalues are typically referred to as outlier eigenvalues in the literature. The detailed proof is provided in Appendix A.2 and is similar to the proof in Baskerville et al. (2022).

Stable rank To compare the rank properties of Hessians of a client and a server, we introduce the concept of stable rank, defined as the square of the ratio between the Frobenius norm and the spectral norm of a matrix \mathbf{A} :

$$\text{srank}(\mathbf{A}) = \frac{\|\mathbf{A}\|_F^2}{\|\mathbf{A}\|_2^2} = \frac{\sum_{i=1}^n \sigma_i^2(\mathbf{A})}{\sigma_1^2(\mathbf{A})} \quad (8)$$

where n is the rank of the matrix \mathbf{A} and $\sigma_i(\mathbf{A})$ is the i -th singular value of the matrix \mathbf{A} . Stable rank serves as a continuous proxy for $\text{rank}(\mathbf{A})$ and is known for its robustness against small perturbations. In fact, stable rank—which emphasizes eigenvalues near the top eigenvalue—can be considered a more accurate surrogate of the rank structure of the Hessian considering the empirical evidences that gradients are highly influenced by the top Hessian eigenvector, i.e., the eigenvectors corresponding to the largest eigenvalues. Additionally, bounds on the stable rank of a weight provide control over the model’s complexity (Georgiev et al., 2021).

In the following theorem, we demonstrate that smaller datasets result in a higher limiting stable rank. Furthermore, given that modern neural network models typically possess a very large number of parameters, this finding is likely applicable to contemporary models.

Theorem 3.3 (Higher rank nature of Hessian of smaller dataset). *Let $N > M > \bar{R}$ be any integers where \bar{R} is the smallest integer such that $\Omega^{\bar{R}}(\theta_1, \dots, \theta_{p+q})$ is non-empty. For any pair $(h^R, \omega^R) \in \Omega^R(\theta_1, \dots, \theta_{p+q})$, let $\mathbf{H}_N(h^R, \omega^R)$ and $\mathbf{H}_M(h^R, \omega^R)$ be the Hessians as defined previously. The difference in stable rank between $\mathbf{H}_N(h^R, \omega^R)$ and $\mathbf{H}_M(h^R, \omega^R)$ converges weakly almost surely to positive value $S(\theta_1, \dots, \theta_{p+q}, \mu) > 0$ as $R \rightarrow \infty$, i.e.*

$$\text{srank}(\mathbf{H}_M(h^R, \omega^R)) - \text{srank}(\mathbf{H}_N(h^R, \omega^R)) \rightarrow S(\theta_1, \dots, \theta_{p+q}, \mu) > 0. \quad (9)$$

Here, the value $S(\theta_1, \dots, \theta_{p+q}, \mu)$ does not depend on the sequence (h^R, ω^R) .

In federated learning, Theorem 3.3 implies that individual clients, often working with smaller, heterogeneous datasets, inherently possess a higher rank structure in their local Hessians compared to the Hessian of the server loss. This higher rank structure can lead to larger discrepancies across clients, as the complexity

and variability in the local training landscapes are greater. Consequently, the optimization paths taken by different clients may diverge more significantly, complicating the aggregation process and potentially degrading the overall performance of the global model. This theoretical insight from Theorem 3.3 is further supported by our empirical findings, as shown in Figure 2.

Understanding this phenomenon is crucial for developing more effective federated learning algorithms. By acknowledging the higher rank structure of client’s Hessian, constraining the rank of client-side optimization can mitigate the discrepancies, especially when local dataset sizes are very small. In the subsequent section, we propose an algorithm that exploits this insight.

3.2 Federated Low-Rank Update(FedLoRU) Algorithm

In this section, we introduce the Federated Low-Rank Updates (FedLoRU) algorithm, along with its variants designed to adapt to statistical and model heterogeneity.

Consider a federated learning system with K clients, where each client k has its own loss function $f^{(k)} : \mathbb{R}^{m \times n} \rightarrow \mathbb{R}$. In conventional federated learning algorithms such as FedAvg (McMahan et al., 2017), the server aims to find a global model $\mathbf{W} \in \mathbb{R}^{m \times n}$ that minimizes the aggregated loss function $f(\mathbf{W}) = \sum_{k=1}^K p^{(k)} f^{(k)}(\mathbf{W})$, where $p^{(k)}$ is the weight of client k . During each round t , the server selects a set of M clients \mathcal{K}_M to participate in local training. These clients receive the global model \mathbf{W}_{t-1} from the server and perform local training without altering the network architecture. The server then receives the locally updated models $\mathbf{W}_t^{(k)}$ from the clients and aggregates them into a global model by averaging: $\mathbf{W}_t = \sum_{k \in \mathcal{K}_M} p^{(k)} \mathbf{W}_t^{(k)}$.

Federated low-rank update algorithm To enhance communication efficiency, FedLoRU constraints clients’ updates to low-rank. Analogous to LoRA (Hu et al., 2021) approach, upon receiving the global model $\mathbf{W} \in \mathbb{R}^{m \times n}$, each client k freezes this model and performs local training through low-rank matrices $\mathbf{A}^{(k)} \in \mathbb{R}^{m \times r}$ and $\mathbf{B}^{(k)} \in \mathbb{R}^{r \times n}$ by solving:

$$\mathbf{A}^{(k)}, \mathbf{B}^{(k)} = \arg \min_{\mathbf{A}, \mathbf{B}} f^{(k)}(\mathbf{W}^{(k)} + \alpha \mathbf{A} \mathbf{B}) \quad (10)$$

where α is a fixed scaling hyperparameter. In FedLoRU, each client solves (10) for E epochs in each round. The server then collects $\mathbf{A}^{(k)}$ and $\mathbf{B}^{(k)}$ from the clients and aggregates them by averaging: $\mathbf{A} = \sum_{k \in \mathcal{K}_M} p^{(k)} \mathbf{A}^{(k)}$, $\mathbf{B} = \sum_{k \in \mathcal{K}_M} p^{(k)} \mathbf{B}^{(k)}$. After aggregation, the server broadcasts the averaged \mathbf{A} and \mathbf{B} to the clients, who continue local training using these matrices.

Occasionally, the server accumulates local updates into the global model after aggregation to achieve a higher-rank global model. Clients subsequently update their local global models by $\mathbf{W}^{(k)} \leftarrow \mathbf{W}^{(k)} + \alpha \mathbf{A} \mathbf{B}$ and reset their low-rank matrices. When we accumulate low-rank updates every τ rounds from the initial global model \mathbf{W}_0 , the final global model at T is

$$\mathbf{W}_T = \mathbf{W}_0 + \sum_{\substack{t=1 \\ t \bmod \tau=0}}^T \mathbf{A}_t \mathbf{B}_t \quad (11)$$

We employ two strategies for initializing the low-rank update matrices in FedLoRU. For random initialization, we initialize \mathbf{A} with a random Gaussian distribution and set \mathbf{B} to zero, ensuring that $\mathbf{A} \mathbf{B}$ is zero at the start. Alternatively, for momentum initialization, we retain the existing weights of the matrices, continuing to use the previous low-rank update matrices. This approach leverages momentum effects as described in the ReLoRA(Lialin et al., 2023). The scheduling of accumulations is also critical due to the varying nature of the training phases across different rounds; in this study, we employ periodic accumulation, though this area warrants further investigation.

Communication overhead FedLoRU reduces communication overhead from Kmn to Kmn when $r \ll m$ or n . While we use a low-rank factorized model here, other options like LoKr or LoHa can be employed, differing only in the factorization scheme but maintaining identical fundamental principles. Additionally, without a compression process, there is no extra computation compared to conventional compression-based communication-efficient federated learning algorithms.

Algorithm 1 FedLoRU. \mathbf{W} is a model, $\mathbf{A}_0, \mathbf{B}_0$ are initial low-rank update matrices, α is a scaling factor, τ is an accumulation cycle, T is the total training round

Require: $\mathbf{W}, \mathbf{A}_0, \mathbf{B}_0, \alpha, \tau, T$

Initialize: Server sends \mathbf{W} to each client, where client k initializes it as $\mathbf{W}^{(k)}$

for $t = 1, \dots, T$ **do**

Server selects M clients \mathcal{K}_M and distributes $\mathbf{A}_{t-1}, \mathbf{B}_{t-1}$ to clients in \mathcal{K}_M

for each client $k \in \mathcal{K}_M$ **do**

Local training: Find $\mathbf{A}_t^{(k)}, \mathbf{B}_t^{(k)}$ by solving (10) starting from $\mathbf{A}_{t-1}, \mathbf{B}_{t-1}$

Send $\mathbf{A}_t^{(k)}, \mathbf{B}_t^{(k)}$ to the server

end for

Server aggregation: $\mathbf{A}_t \leftarrow \sum_{k \in \mathcal{K}_M} p^{(k)} \mathbf{A}_t^{(k)}, \mathbf{B}_t \leftarrow \sum_{k \in \mathcal{K}_M} p^{(k)} \mathbf{B}_t^{(k)}$

if $t \bmod \tau = 0$ **then**

Server distributes $\mathbf{A}_t, \mathbf{B}_t$ to all clients

Each client k updates its local model: $\mathbf{W}^{(k)} \leftarrow \mathbf{W}^{(k)} + \alpha \mathbf{A}_t \mathbf{B}_t$

end if

end for

Return: $\mathbf{W} + \alpha \sum_{t=1: t \bmod \tau=0}^T \mathbf{A}_t \mathbf{B}_t$

Low-rank local training, higher-rank global training, and implicit regularization Moreover, FedLoRU facilitates the training of a higher-rank global model concurrently with low-rank local updates. With each accumulation of low-rank update matrices, the global model’s rank is incrementally enhanced, enabling the initiation of new learning phases. This process is evident in the training curve, which exhibits noticeable pattern shifts following each accumulation. Moreover, constraining the rank of local training introduces a regularization effect, thereby diminishing the discrepancy between updated local models.

Federated low-rank update for statistical heterogeneous setting We develop the personalized FedLoRU (pFedLoRU) algorithm to address statistical heterogeneity in federated learning using low-rank updates idea. In pFedLoRU, each client k maintains a global model \mathbf{W} , global low-rank matrices $\mathbf{A}^{(k)}$ and $\mathbf{B}^{(k)}$, and personal low-rank matrices $\mathbf{L}^{(k)}$ and $\mathbf{U}^{(k)}$. The matrices $\mathbf{A}^{(k)}$ and $\mathbf{B}^{(k)}$ are shared between the server and clients to update common global model, while $\mathbf{L}^{(k)}$ and $\mathbf{U}^{(k)}$ are tailored to adapt to the local distribution. In each round t , client k optimizes the personal matrices for E_{per} epochs and the global matrices for E_{global} by solving:

$$\mathbf{L}_t^{(k)}, \mathbf{U}_t^{(k)} = \arg \min_{\mathbf{L}, \mathbf{U}} f^{(k)}(\mathbf{W}^{(k)} + \alpha_{\text{global}} \mathbf{A}_{t-1}^{(k)} \mathbf{B}_{t-1}^{(k)} + \alpha_{\text{per}} \mathbf{L} \mathbf{U}) \quad (12)$$

$$\mathbf{A}_t^{(k)}, \mathbf{B}_t^{(k)} = \arg \min_{\mathbf{A}, \mathbf{B}} f^{(k)}(\mathbf{W}^{(k)} + \alpha_{\text{global}} \mathbf{A} \mathbf{B} + \alpha_{\text{per}} \mathbf{L}_t^{(k)} \mathbf{U}_t^{(k)}) \quad (13)$$

Subsequently, the server collects the global update matrices from the clients, performs aggregation, and updates the global model accordingly. A detailed description of the pFedLoRU algorithm can be found in Appendix B.

Federated low-rank update for model heterogeneous setting When local clients possess varying hardware resources and communication speeds, it becomes impractical to use uniform low-rank matrices across all clients. To address this issue, we develop the model-heterogeneous FedLoRU (mFedLoRU) algorithm, which employs hierarchical low-rank updates. Specifically, to update the low-rank matrices \mathbf{A} and \mathbf{B} , we apply low-rank updates recursively, enabling model adaptation through nested low-rank updates:

$$\mathbf{A} \mathbf{B} \leftarrow (\mathbf{A} + \alpha_A \mathbf{A}_d \mathbf{A}_u)(\mathbf{B} + \alpha_B \mathbf{B}_d \mathbf{B}_u) \quad (14)$$

Here, $\mathbf{A} \mathbf{B}$ is the rank- r factorization of a matrix $\mathbf{W} \in \mathbb{R}^{m \times n}$, and $\mathbf{A}_d \mathbf{A}_u$ and $\mathbf{B}_d \mathbf{B}_u$ are rank- r_A and rank- r_B factorizations of \mathbf{A} and \mathbf{B} , respectively. In mFedLoRU, each client k decides whether to use nested low-rank updates and, if so, determines the locally adapted rank $r^{(k)}$ based on its resources. If a client opts out of nested low-rank updates, it updates its low-rank modules like in FedLoRU. However, if it chooses nested low-rank updates, it generates and optimizes the nested low-rank matrices $\mathbf{A}_d \mathbf{A}_u$ and $\mathbf{B}_d \mathbf{B}_u$ by solving:

Dataset	Data setting	#clients	FedAvg		FedLoRA		FedHM		FedLoRU	
			#params	acc	#params	acc	#params	acc	#params	acc
CIFAR-10	IID	K=20	11.17M	93.48	4.59M	91.65	4.59M	90.76	4.59M	92.43
							3.44M	90.32	3.44M	90.71
		K=100	11.17M	85.14	4.59M	79.48	4.59M	81.41	4.59M	81.36
							3.44M	81.58	3.44M	86.01
	Non-IID	K=20	11.17M	79.65	4.59M	69.60	4.59M	70.55	4.59M	75.19
							3.44M	66.39	3.44M	69.71
		K=100					2.30M	65.48	2.30M	67.88
							2.30M	82.12	2.30M	86.10
CIFAR-100	IID	K=20	11.22M	69.97	4.63M	65.53	4.63M	59.43	4.63M	66.81
							3.49M	58.40	3.49M	60.78
		K=100	11.22M	55.14	4.63M	39.44	4.63M	40.88	4.63M	57.76
							3.49M	40.04	3.49M	53.25
	Non-IID	K=20					2.35M	40.82	2.35M	53.53
							2.35M	40.82	2.35M	53.53
		K=100	11.22M	19.18	4.63M	14.41	4.63M	16.88	4.63M	16.46
							3.49M	15.04	3.49M	13.70
				2.35M	15.13	2.35M	14.52			

Table 1: Top-1 test accuracy comparison with different communication-efficient federated learning methods under various FL settings.

$$\mathbf{A}_d^{(k)}, \mathbf{A}_u^{(k)}, \mathbf{B}_d^{(k)}, \mathbf{B}_u^{(k)} = \arg \min_{\mathbf{A}_d, \mathbf{A}_u, \mathbf{B}_d, \mathbf{B}_u} f^{(k)}(\mathbf{W}^{(k)} + \alpha(\mathbf{A} + \alpha_A^{(k)} \mathbf{A}_d \mathbf{A}_u)(\mathbf{B} + \alpha_B^{(k)} \mathbf{B}_d \mathbf{B}_u)) \quad (15)$$

After local training, client k sends its nested low-rank matrices to the server, which recovers them into rank- r low-rank matrices $\mathbf{A}^{(k)} \leftarrow \mathbf{A} + \alpha_A^{(k)} \mathbf{A}_d^{(k)} \mathbf{A}_u^{(k)}$, and $\mathbf{B}^{(k)} \leftarrow \mathbf{B} + \alpha_B^{(k)} \mathbf{B}_d^{(k)} \mathbf{B}_u^{(k)}$, and then performs aggregation using these rank- r low-rank matrices as in FedLoRU. A detailed description of the mFedLoRU algorithm can be found in Appendix B.

4 Experiments

In this section, we extensively evaluate FedLoRU on pre-training and fine-tuning on different heterogeneous settings. We first provide the experiment setup such as baselines and heterogeneous settings, then move on to the performance evaluation.

4.1 Experiment setup

Datasets and Models To evaluate the performance of our proposed algorithms, we employ three commonly used datasets in machine learning: CIFAR-10, CIFAR-100 (Krizhevsky et al., 2009), and Alpaca (Taori et al., 2023). For the image datasets, we employ ResNet-18 (He et al., 2016) as the model architecture, and for the language dataset, we use LLaMa2-3B (Touvron et al., 2023). In pre-training experiments on the image datasets, we vary the number of clients between 20 and 400 to evaluate the algorithms under diverse conditions and to investigate the effect of client numbers. At each round, 50% of the clients are randomly sampled to train models over 5 local epochs. For fine-tuning the language model, we configure 10 clients with a 50% participation rate and conduct training for 1 local epoch. The learning rate is selected through grid search, and various rank configurations are tested for FedHM and FedLoRU.

Baseline Algorithms We conduct a comparative analysis of FedLoRU against several benchmarks: FedAvg, the standard federated learning algorithm that trains full-rank models; FedLoRA, which trains low-rank modules without accumulating low-rank updates; and FedHM, the state-of-the-art in communication-efficient federated learning. For evaluating pFedLoRU, we compare it with pFedLoRA, and for mFedLoRU, we use the system-heterogeneous version of FedHM as the comparison baseline.

Heterogeneous Settings In the statistically heterogeneous setting, we generate disjoint Non-IID client data using a Dirichlet distribution, $\text{Dir}(\alpha)$, with a concentration parameter α set to 0.5, as described in Hsu et al. (2019). For the system heterogeneous setting, we simulate virtual environments where each client is assigned a different level of computational complexity, thereby restricting them to use low-rank update matrices of varying ranks. The specific configurations for these settings are detailed in Appendix C.

4.2 Performance Evaluation

We evaluate the Top-1 accuracy of models with varying parameter sizes in both IID and Non-IID scenarios across different federated learning configurations.

Performance of Pre-training Table 1 shows the performance of FedLoRU and baseline algorithms. In our experimental evaluation, FedLoRU consistently achieves competitive or superior accuracy compared to other algorithms, demonstrating its effectiveness in federated learning environments. While FedLoRU exhibits slightly lower performance compared to FedAvg in most settings, the performance degradation is minimal when considering the significantly reduced number of parameters. This indicates that FedLoRU’s low-rank update and accumulation strategy effectively reduces communication overhead without substantially sacrificing model performance. Moreover, FedLoRU surpasses other communication-efficient federated learning algorithms.

The client regularization effect of FedLoRU, as predicted by our theoretical analysis, suggests that using client-side low-rank updates is particularly beneficial in environments with a large number of clients. This benefit is evident in experiments under IID conditions with 100 clients, where FedLoRU attains the highest accuracy among the tested methods. Furthermore, under Non-IID settings, all methods experience considerable performance degradation compared to the IID setting; however, FedAvg still exhibits the best performance. However, as we will discuss in subsequent sections, the challenge of statistical heterogeneity can be addressed by utilizing personalized federated learning algorithms, and pFedLoRU surpasses the state-of-the-art personalized FL algorithms.

Performance of LLM Fine-tuning Figure 3 presents the loss curves of FedLoRA and FedLoRU during the fine-tuning of a LLaMA2-3B model on the Alpaca dataset. The train loss curves show that both algorithms achieve similar convergence rates, with minimal differences in training optimization. However, a notable distinction emerges in the test loss results, where FedLoRU consistently outperforms FedLoRA after the 25th communication round.

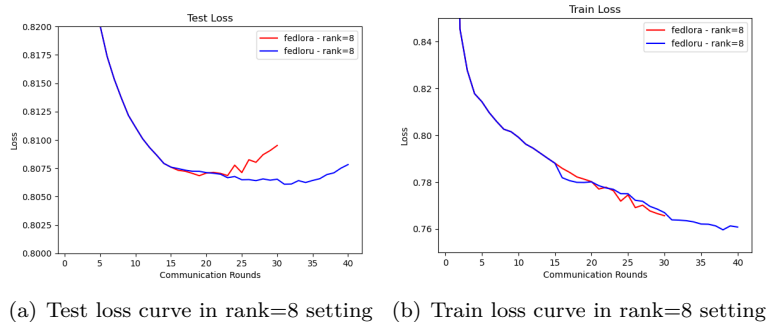


Figure 3: Loss curve comparison of FedLoRU and FedLoRA for fine-tuning LLaMa2-3B on Alpaca dataset in rank=8 setting.

In this fine-tuning experiment, we accumulate the results every 15 communication rounds. Notably, despite FedLoRU performing an additional accumulation at round 30, the test loss does not show any further improvement. This suggests that beyond a certain point, further accumulation may not necessarily enhance the model’s generalization performance.

Scalability and Performance of FedLoRU in Large-Client Federated Learning As the number of clients in federated learning increases, the scalability and performance of algorithms become critical. Our experiments reveal that FedAvg’s performance drops drastically as the number of clients grows—from a Top-1 accuracy of 69.97% at $K = 20$ to just 21.44% at $K = 400$. This sharp decline suggests that FedAvg struggles to maintain model accuracy in large-scale federated learning environments.

In contrast, FedLoRU outperforms FedAvg as the number of clients increases. While FedAvg slightly outperforms FedLoRU with smaller numbers of clients ($K = 20$ and $K = 50$), FedLoRU consistently surpasses FedAvg when the client count ranges from $K = 100$ to $K = 400$. Moreover, the performance gap widens with larger client numbers, indicating that FedLoRU scales more effectively with a higher number

K	FedAvg	FedLoRU	Ratio
20	69.97	66.81	-0.046
50	64.68	62.45	-0.034
100	55.14	57.76	0.048
200	38.85	42.55	0.095
300	24.94	33.81	0.356
400	21.44	33.25	0.551

Table 2: Comparison of FedAvg and FedLoRU with different K (number of clients) values and corresponding ratios.

of clients—an essential feature for large-scale federated learning scenarios. To quantify the performance difference, we define the ratio:

$$\text{Ratio} = \frac{\text{FedLoRU} - \text{FedAvg}}{\text{FedLoRU}}$$

This ratio represents the relative decrease in accuracy when using FedAvg instead of FedLoRU, expressed as a proportion of FedLoRU’s accuracy. Higher ratio values with increasing K highlight FedLoRU’s superior scalability and effectiveness in environments with extensive client participation.

Performance of pFedLoRU and mFedLoRU In our experiments, we evaluate the performance of pFedLoRU and mFedLoRU on statistical heterogeneous and system heterogeneous FL environments. Table 3 shows the performance of pFedLoRU and pFedLoRA. Under both non-IID levels ($\alpha = 0.1$ and $\alpha = 0.5$), pFedLoRU shows a clear advantage in terms of accuracy compared to pFedLoRA. In addition, despite having less than half the number of parameters, pFedLoRU consistently achieves higher accuracy.

Dataset	α	pFedLoRA(1)		pFedLoRA(2)		pFedLoRU	
		#params	acc	#params	acc	#params	acc
CIFAR100	0.1	11.22M	45.36	11.22M	47.45	4.63M	49.65
	0.5	11.22M	42.14	11.22M	42.28	4.63M	46.50

Table 3: Comparison of pFedLoRA and pFedLoRU with varying non-iidness (α) on CIFAR100 dataset.

Dataset	Heterogeneous Setting	FedHM	mFedLoRU
CIFAR-10	setting 1	88.09	84.81
	setting 2	88.68	84.36
CIFAR-100	setting 1	49.84	51.16
	setting 2	50.52	50.89

Table 4: Comparison of FedHM and mFedLoRU in two system-heterogeneous setting.

On the other hands, Table 4 shows the performanec of mFedLoRU and FedHM. FedHM outperforms mFedLoRU in both heterogeneous settings (setting 1 and setting 2) for the CIFAR-10 dataset, indicating that FedHM handles model heterogeneity more effectively for simpler tasks. This suggests that FedHM is better suited for less complex datasets such as CIFAR-10, where its approach proves more efficient. However, mFedLoRU outperforms FedHM in both heterogeneous settings for the more complex CIFAR-100 dataset, demonstrating its potential in addressing the model-heterogeneous problem in federated learning. A key advantage of mFedLoRU is that it does not require additional computational steps, such as the weight factorization used in FedHM, making it a more efficient solution in scenarios involving more challenging tasks.

5 Conclusion

In conclusion, FedLoRU demonstrates comparable performance to FedAvg while utilizing significantly fewer trainable and communicated parameters. This highlights its efficiency in reducing communication overhead

without sacrificing accuracy. Furthermore, as the number of clients increases, FedLoRU consistently outperforms FedAvg, even though it operates with a much smaller parameter set. This scalability makes FedLoRU an effective solution for federated learning in large-scale environments, maintaining strong performance under more challenging conditions.

We also introduce two variants of the FedLoRU algorithm: pFedLoRU and mFedLoRU. These variants perform particularly well in heterogeneous environments, demonstrating their potential for broader applicability across various federated learning settings. However, a key limitation of FedLoRU lies in determining the optimal accumulation schedule for low-rank updates. The performance of the algorithm is highly dependent on the timing of these accumulations, and finding the best schedule can be challenging. Testing multiple accumulation schedules is not efficient, and thus, future research should focus on developing methods to optimize or automate this process.

References

- Azam, S. S., Hosseinalipour, S., Qiu, Q., and Brinton, C. (2021). Recycling model updates in federated learning: Are gradient subspaces low-rank? In *International Conference on Learning Representations*.
- Baskerville, N. P., Keating, J. P., Mezzadri, F., Najnudel, J., and Granzio, D. (2022). Universal characteristics of deep neural network loss surfaces from random matrix theory. *Journal of Physics A: Mathematical and Theoretical*, 55(49):494002.
- Benaych-Georges, F. and Nadakuditi, R. R. (2011). The eigenvalues and eigenvectors of finite, low rank perturbations of large random matrices. *Advances in Mathematics*, 227(1):494–521.
- Caldas, S., Konečný, J., McMahan, H. B., and Talwalkar, A. (2018). Expanding the reach of federated learning by reducing client resource requirements. *arXiv preprint arXiv:1812.07210*.
- Cho, Y. J., Liu, L., Xu, Z., Fahrezi, A., Barnes, M., and Joshi, G. (2023). Heterogeneous lora for federated fine-tuning of on-device foundation models. In *International Workshop on Federated Learning in the Age of Foundation Models in Conjunction with NeurIPS 2023*.
- Dettmers, T., Pagnoni, A., Holtzman, A., and Zettlemoyer, L. (2024). Qlora: Efficient finetuning of quantized llms. *Advances in Neural Information Processing Systems*, 36.
- Georgiev, B., Franken, L., Mukherjee, M., and Arvanitidis, G. (2021). On the impact of stable ranks in deep nets. *arXiv preprint arXiv:2110.02333*.
- Granzio, D., Zohren, S., and Roberts, S. (2022). Learning rates as a function of batch size: A random matrix theory approach to neural network training. *Journal of Machine Learning Research*, 23(173):1–65.
- Gur-Ari, G., Roberts, D. A., and Dyer, E. (2018). Gradient descent happens in a tiny subspace. *arXiv preprint arXiv:1812.04754*.
- He, K., Zhang, X., Ren, S., and Sun, J. (2016). Deep residual learning for image recognition. In *Proceedings of the IEEE conference on computer vision and pattern recognition*, pages 770–778.
- Hsu, T.-M. H., Qi, H., and Brown, M. (2019). Measuring the effects of non-identical data distribution for federated visual classification. *arXiv preprint arXiv:1909.06335*.
- Hu, E. J., Shen, Y., Wallis, P., Allen-Zhu, Z., Li, Y., Wang, S., Wang, L., and Chen, W. (2021). Lora: Low-rank adaptation of large language models. *arXiv preprint arXiv:2106.09685*.
- Huh, M., Mobahi, H., Zhang, R., Cheung, B., Agrawal, P., and Isola, P. (2021). The low-rank simplicity bias in deep networks. *arXiv preprint arXiv:2103.10427*.
- Jadbabaie, A., Makur, A., and Shah, D. (2023). Federated optimization of smooth loss functions. *IEEE Transactions on Information Theory*.
- Jhunjunwala, D., Gadhikar, A., Joshi, G., and Eldar, Y. C. (2021). Adaptive quantization of model updates for communication-efficient federated learning. In *ICASSP 2021-2021 IEEE International Conference on Acoustics, Speech and Signal Processing (ICASSP)*, pages 3110–3114. IEEE.
- Ji, Z. and Telgarsky, M. (2018). Gradient descent aligns the layers of deep linear networks. *arXiv preprint arXiv:1810.02032*.
- Jiang, Z., Xu, Y., Xu, H., Wang, Z., Liu, J., Chen, Q., and Qiao, C. (2023). Computation and communication efficient federated learning with adaptive model pruning. *IEEE Transactions on Mobile Computing*, 23(3):2003–2021.
- Kairouz, P., McMahan, H. B., Avent, B., Bellet, A., Bennis, M., Bhagoji, A. N., Bonawitz, K., Charles, Z., Cormode, G., Cummings, R., et al. (2021). Advances and open problems in federated learning. *Foundations and trends® in machine learning*, 14(1–2):1–210.
- Krizhevsky, A., Hinton, G., et al. (2009). Learning multiple layers of features from tiny images.

- Kuo, K., Raje, A., Rajesh, K., and Smith, V. (2024). Federated lora with sparse communication. *arXiv preprint arXiv:2406.05233*.
- Li, C., Farkhoor, H., Liu, R., and Yosinski, J. (2018). Measuring the intrinsic dimension of objective landscapes. *arXiv preprint arXiv:1804.08838*.
- Lialin, V., Muckatira, S., Shivagunde, N., and Rumshisky, A. (2023). Relora: High-rank training through low-rank updates. In *The Twelfth International Conference on Learning Representations*.
- Loshchilov, I. (2017). Decoupled weight decay regularization. *arXiv preprint arXiv:1711.05101*.
- Lu, Q., Niu, D., Khoshkho, M. S., and Li, B. (2024). Hyperflora: Federated learning with instantaneous personalization. In *Proceedings of the 2024 SIAM International Conference on Data Mining (SDM)*, pages 824–832. SIAM.
- McMahan, B., Moore, E., Ramage, D., Hampson, S., and y Arcas, B. A. (2017). Communication-efficient learning of deep networks from decentralized data. In *Artificial intelligence and statistics*, pages 1273–1282. PMLR.
- Pielaszekiewicz, J. and Singull, M. (2015). Closed form of the asymptotic spectral distribution of random matrices using free independence.
- Qiao, Z., Yu, X., Zhang, J., and Letaief, K. B. (2021). Communication-efficient federated learning with dual-side low-rank compression. *arXiv preprint arXiv:2104.12416*.
- Reisizadeh, A., Mokhtari, A., Hassani, H., Jadbabaie, A., and Pedarsani, R. (2020). Fedpaq: A communication-efficient federated learning method with periodic averaging and quantization. In *International conference on artificial intelligence and statistics*, pages 2021–2031. PMLR.
- Sagun, L., Bottou, L., and LeCun, Y. (2016). Eigenvalues of the hessian in deep learning: Singularity and beyond. *arXiv preprint arXiv:1611.07476*.
- Shahid, O., Pouriye, S., Parizi, R. M., Sheng, Q. Z., Srivastava, G., and Zhao, L. (2021). Communication efficiency in federated learning: Achievements and challenges. *arXiv preprint arXiv:2107.10996*.
- Sun, Y., Li, Z., Li, Y., and Ding, B. (2024). Improving lora in privacy-preserving federated learning. *arXiv preprint arXiv:2403.12313*.
- Taori, R., Gulrajani, I., Zhang, T., Dubois, Y., Li, X., Guestrin, C., Liang, P., and Hashimoto, T. B. (2023). Stanford alpaca: An instruction-following llama model. https://github.com/tatsu-lab/stanford_alpaca.
- Touvron, H., Martin, L., Stone, K., Albert, P., Almahairi, A., Babaei, Y., Bashlykov, N., Batra, S., Bhargava, P., Bhosale, S., et al. (2023). Llama 2: Open foundation and fine-tuned chat models. *arXiv preprint arXiv:2307.09288*.
- Valipour, M., Rezagholizadeh, M., Kobzyev, I., and Ghodsi, A. (2022). Dylora: Parameter efficient tuning of pre-trained models using dynamic search-free low-rank adaptation. *arXiv preprint arXiv:2210.07558*.
- Wu, X., Liu, X., Niu, J., Wang, H., Tang, S., and Zhu, G. (2024). Fedlora: When personalized federated learning meets low-rank adaptation.
- Yao, D., Pan, W., O’Neill, M. J., Dai, Y., Wan, Y., Jin, H., and Sun, L. (2021). Fedhm: Efficient federated learning for heterogeneous models via low-rank factorization. *arXiv preprint arXiv:2111.14655*.
- Yao, Z., Gholami, A., Keutzer, K., and Mahoney, M. W. (2020). Pyhessian: Neural networks through the lens of the hessian. In *2020 IEEE international conference on big data (Big data)*, pages 581–590. IEEE.
- Ye, M., Fang, X., Du, B., Yuen, P. C., and Tao, D. (2023). Heterogeneous federated learning: State-of-the-art and research challenges. *ACM Computing Surveys*, 56(3):1–44.
- Ye, R., Wang, W., Chai, J., Li, D., Li, Z., Xu, Y., Du, Y., Wang, Y., and Chen, S. (2024). Openfedllm: Training large language models on decentralized private data via federated learning. *arXiv preprint arXiv:2402.06954*.
- Yi, L., Yu, H., Wang, G., and Liu, X. (2023). Fedlora: Model-heterogeneous personalized federated learning with lora tuning. *arXiv preprint arXiv:2310.13283*.
- Yu, H. and Wu, J. (2023). Compressing transformers: features are low-rank, but weights are not! In *Proceedings of the AAAI Conference on Artificial Intelligence*, volume 37, pages 11007–11015.
- Zhao, J., Zhang, Z., Chen, B., Wang, Z., Anandkumar, A., and Tian, Y. (2024). Galore: Memory-efficient llm training by gradient low-rank projection. *arXiv preprint arXiv:2403.03507*.
- Zheng, S., Shen, C., and Chen, X. (2020). Design and analysis of uplink and downlink communications for federated learning. *IEEE Journal on Selected Areas in Communications*, 39(7):2150–2167.

A Proof of the main theorem

In this section, we provide proofs of Proposition 3.1 Proposition 3.2 and Theorem 3.3. We begin by presenting some lemmas that will be required for our analysis, then proceed to prove the propositions and the theorem.

Lemma A.1 (Theorem 2.2 from Pielaszkiwicz and Singull (2015)). *Let μ_n be a sequence of probability measures on \mathbb{R} and let g_{μ_n} denote the Stieltjes transform of μ_n . Then*

- a) *if $\mu_n \rightarrow \mu$ weakly, where μ is a measure on \mathbb{R} , then $g_{\mu_n}(z) \rightarrow g_{\mu}(z)$ pointwise for any $z \in \{z : z \in \mathbb{C}, \Im(z) > 0\}$*
- b) *if $g_{\mu_n}(z) \rightarrow g(z)$ pointwise, for all $z \in \{z : z \in \mathbb{C}, \Im(z) > 0\}$, then there exists a unique non-negative and finite measure such that $g = g_{\mu}$ and $\mu_n \rightarrow \mu$ weakly*

Lemma A.2 (Theorem 3.4 from Baskerville et al. (2022)). *Let X be an $N \times N$ real symmetric random matrix and let D be an $N \times N$ symmetric matrix (deterministic or random). Let $\hat{\mu}_X, \hat{\mu}_D$ be the empirical spectral measures of the sequence of matrices X, D and assume there exist deterministic limit measures μ_X, μ_D . Assume that X has QUE and $\hat{\mu}_X$ concentrates in the sense that*

$$\mathbb{P}(W_1(\hat{\mu}_X, \mu_X) > \delta) \leq e^{-N^\tau f(\delta)}$$

where $\tau > 0$ and f is some positive increasing function. Then $H = X + D$ has a limiting spectral measure and it is given by the free convolution $\mu_X \boxplus \mu_D$

Lemma A.3 (Weyl's inequality). *For Hermitian matrices $\mathbf{A}, \mathbf{B} \in \mathbb{C}^{R \times n}$ and $i, j \in \{1, \dots, n\}$,*

$$\lambda_{i+j-1}(\mathbf{A} + \mathbf{B}) \leq \lambda_i(\mathbf{A}) + \lambda_j(\mathbf{B}), \quad i + j \leq n + 1, \quad (16)$$

$$\lambda_{i+j-n}(\mathbf{A} + \mathbf{B}) \geq \lambda_i(\mathbf{A}) + \lambda_j(\mathbf{B}), \quad i + j \geq n + 1, \quad (17)$$

where $\lambda_i(\mathbf{A})$ is i -th eigenvalue of \mathbf{A} .

A.1 Proof of Proposition 3.1

Suppose $(h^{\tilde{R}}, \omega^{\tilde{R}}) \in \Omega^{\tilde{R}}(\theta_1, \dots, \theta_k)$, i.e., $\mathbf{H}_{\text{true}}(h^{\tilde{R}}, \omega^{\tilde{R}})$ has non-zero eigenvalues $\theta_1, \dots, \theta_k$. To construct a prediction function $h^{\tilde{R}+1}$ and a weight $\omega^{\tilde{R}+1}$ of dimension $\tilde{R} + 1$ such that the true Hessian retains the same non-zero eigenvalues, define:

$$h^{\tilde{R}+1}(\omega^{\tilde{R}}, z) = h^{\tilde{R}}(\omega^{\tilde{R}}) + g^{\tilde{R}+1}(\omega^{\tilde{R}}, z) \quad (18)$$

$$\omega^{\tilde{R}+1} = (\omega^{\tilde{R}}, z) \quad (19)$$

where $\nabla^2 \int \ell(g^{\tilde{R}+1}(\mathbf{x}; (\omega^{\tilde{R}}, z)), \mathbf{y}) d\psi(\mathbf{x}, \mathbf{y}) = 0$ ensures that the second derivative with respect to the new function $g^{\tilde{R}+1}$ vanishes. Thus, since $h^{\tilde{R}+1}$ and $h^{\tilde{R}}$ share the same true Hessian, it follows that $(h^{\tilde{R}+1}, \omega^{\tilde{R}+1}) \in \Omega^{\tilde{R}+1}(\theta_1, \dots, \theta_k)$. Specifically, if we consider feed-forward neural networks as prediction functions, one can easily construct a larger neural network that maintains the same non-zero eigenvalues by adding an additional neuron with a single connection to a neuron in the previous layer. This additional neuron does not affect the final output, thereby preserving the desired eigenvalue properties.

A.2 Proof of Proposition 3.2

To prove Proposition 3.2, we decompose the eigenvalue analysis into two distinct parts. First, we demonstrate that the i -th eigenvalues, where $i \in \{p + 1, \dots, P - q - 1\}$, converge to the upper or lower bounds of the spectral density of μ_N . This portion of the proof parallels the approach employed by Benaych-Georges and Nadakuditi (2011). Second, we show that the remaining eigenvalues converge to the Stieltjes transformation. This part of the proof follows the methodology outlined by Baskerville et al. (2022).

Proof. In the proof, we drop dependency on (h^R, ω^R) since it is clear. First, consider $\lambda_i(\mathbf{H}_N)$ where $p < i < R - q$. By using Lemma A.3, we have

$$\lambda_i(\mathbf{H}_N) \leq \lambda_{1+i-j}(\mathbf{H}_{\text{true}}) + \lambda_{1+i-k}(\epsilon(N)), \quad i \leq R, \quad i = j + k - 1, \quad j, k \in \{1, \dots, R\} \quad (20)$$

$$\lambda_i(\mathbf{H}_N) \leq \lambda_{R+i-j}(\mathbf{H}_{\text{true}}) + \lambda_{R+i-k}(\epsilon(N)), \quad i \geq 1, \quad i = j + k - R, \quad j, k \in \{1, \dots, R\} \quad (21)$$

If we put $k = 1 + p$ on (20) and $k = R - q$ on (21), since $\lambda_{1+p}(\mathbf{H}_{\text{true}}) = 0$ and $\lambda_{R-q}(\mathbf{H}_{\text{true}}) = 0$, we deduce

$$\lambda_{i+q}(\epsilon(N)) \leq \lambda_i(H_N) \leq \lambda_{i-p}(\epsilon(N)), \quad \forall i \in \{1, \dots, R\} \quad (22)$$

where $\lambda_k(\epsilon(N)) = -\infty$ if $k > R$ and $+\infty$ if $k \leq 0$. Additionally, since $\epsilon(N)$ has the limiting spectral density μ_N and L_N, U_N are lower and upper bound of μ_N , we have for all $1 \leq i \leq R$,

$$\liminf_{R \rightarrow \infty} \lambda_i(\epsilon(N)) \geq U_N \quad \text{and} \quad \limsup_{R \rightarrow \infty} \lambda_{R+1-i}(\epsilon(N)) \leq L_N \quad (23)$$

$$\lambda_1(\epsilon(N)) \rightarrow U_N \quad \text{and} \quad \lambda_R(\epsilon(N)) \rightarrow L_N \quad (24)$$

From the above relations, it follows that for all fixed $1 \leq i \leq R$, $\lambda_i(\epsilon(N)) \rightarrow U_N$ and $\lambda_{R+1-i}(\epsilon(N)) \rightarrow L_N$. By (22), we have

$$\liminf_{n \rightarrow \infty} \lambda_i(H_N) \geq U_N \quad \text{and} \quad \limsup_{n \rightarrow \infty} \lambda_i(H_N) \leq L_N \quad (25)$$

and for all $i > p$ (resp. $i \geq q$) fixed, we have

$$\lambda_i(H_N) \rightarrow U_N \quad (\text{resp. } \lambda_{R-i}(H_N) \rightarrow L_N) \quad (26)$$

Now, we are going to prove the remaining eigenvalues $\lambda_i(\mathbf{H}_N)$, where $i \in \{1, \dots, p, R - q + 1, \dots, R\}$. Note that, since $p + q \ll R$ when R is large enough, the limiting spectral density of H_{true} converges to $\nu = \delta_0$.

Consider $\lambda_i(H_N)$ where $i \leq p$ or $i \geq R - q$. By the Lemma A.2, the limiting spectral density μ_{H_N} of H_N is $\mu_N \boxplus \nu$ where μ_N is the limiting spectral density of $\epsilon(N)$. Then by the Lemma A.1, the Stieltjes transform $g_{\mu_{H_N}}(z)$ converges pointwise to $g_{\nu \boxplus \mu_N}(z)$ for any $z \in \{z : z \in \mathbb{C}, \Im(z) > 0\}$. Therefore, we have

$$\begin{aligned} \widehat{g}_{H_N(h^R, \omega^R)}(z) &= g_{\mu_{H_N}(h^R, \omega^R)}(z) + o(1) \\ &= g_{\mu_N(h^R, \omega^R) \boxplus \nu(h^R, \omega^R)}(z) + o(1) \\ &= g_{\nu(h^R, \omega^R)}(k(z)) + o(1) \\ &= \widehat{g}_{H_{\text{true}}(h^R, \omega^R)}(k(z)) + o(1) \end{aligned} \quad (27)$$

where k is the subordination function such that $g_{\mu_N \boxplus \nu}(z) = g_{\nu}(k(z))$.

Let $\lambda \in \mathbb{R} \setminus \text{supp}(\mu_N \boxplus \nu)$ be an eigenvalue of H_N . Then \widehat{g}_{H_N} has a singularity at λ , thus $\widehat{g}_{H_{\text{true}}}$ has a singularity at $k(\lambda)$, thus, for any R , this singularity should persist and $k(\lambda)$ must coincide with one of the outliers of H_N , i.e., θ_i is an outlier eigenvalue of H_{true} if and only if there exists an eigenvalue λ of H_N contained in $\mathbb{R} \setminus \text{supp}(\mu_N \boxplus \nu)$ such that $k(\lambda) = \theta_i$. Thus, we can write the outliers of H_N as

$$\{k^{-1}(\theta_j) : k^{-1}(\theta_j) \in \mathbb{R} \setminus \text{supp}(\mu_N \boxplus \nu)\} \quad (28)$$

Note that $\text{supp}(\mu_N \boxplus \nu) = \text{supp}(\mu_N \boxplus \delta_0) = \text{supp}(\mu_N)$. Now, we want to find the form of $k^{-1}(\theta_j)$. From the subordination function relation, we have

$$\begin{aligned} k^{-1}(\theta) &= g_{\mu_N \boxplus \nu}^{-1}(g_{\nu}(\theta)) \\ &= \mathcal{R}_{\mu_N}(g_{\nu}(\theta)) + g_{\nu}^{-1}(g_{\nu}(\theta)) \\ &= \mathcal{R}_{\mu_N}(1/\theta) + \theta \end{aligned} \quad (29)$$

Note that by the definition of Stieltjes transformation and \mathcal{R} -transform $g_\nu(\theta) = g_{\delta_0}(\theta) = 1/\theta$.

Let $m_n^{(\mu)}$ be the n -th moment of a distribution μ and $C_n^{(\mu)}$ be the n -th cumulant of μ . Then we have the relationship between $m_n^{(\mu)}$ and $C_n^{(\mu)}$ ([3]) as

$$m_n^{(\mu)} = \sum_{r=1}^n \sum_{\substack{0 \leq i_1, \dots, i_r \leq n-r \\ i_1 + \dots + i_r = n-r}} C_r^{(\mu)} \left[\prod_{j=1}^r m_{i_j}^{(\mu)} \right] \quad (30)$$

Therefore, from the moment's scaling property, $m_n^{\mu_N} = s(N)^n m_n^\mu$, we can deduce the scaling relation property of the cumulants, $C_n^{(\mu_N)} = s(N)^n C_n^{(\mu)}$, therefore we have the scaling property of \mathcal{R} -transform:

$$\mathcal{R}_{\mu_N}(\theta) = s(N) \mathcal{R}_\mu(s(N)\theta) \quad (31)$$

Finally, we have a expression for the outliers of H_N as

$$k^{-1}(\theta) = s(N) \mathcal{R}_\mu(s(N)/\theta) + \theta \quad (32)$$

□

A.3 Proof of Theorem 3.3

Proof. Suppose α and β be the size of sets $\{i > p : \lambda_i(H_N) \rightarrow U_N\}$ and $\{i \geq q : \lambda_{R-i}(H_N) \rightarrow L_N\}$ respectively, and a_N and b_N be integers such that

$$\begin{aligned} g_N^{-1}(\theta_{a_N}) &> U_N > g_N^{-1}(\theta_{a_N+1}) \\ g_N^{-1}(\theta_{p+q-b_N}) &> L_N > g_N^{-1}(\theta_{p+q-b_N+1}) \end{aligned}$$

and we can define a_M and b_M in the similar manner. Then we have

$$\overbrace{\theta_1 > \dots > \theta_{a_N}}^{a_N} > \overbrace{\theta_{a_N+1} > \dots > \theta_p}^{p-a_N} > 0 > \overbrace{\theta_{p+1} > \dots > \theta_{p+q-b_N}}^{q-b_N} > \overbrace{\theta_{p+q-b_N+1} > \dots > \theta_{p+q}}^{b_N} \quad (33)$$

$$\overbrace{\theta_1 > \dots > \theta_{a_M}}^{a_M} > \overbrace{\theta_{a_M+1} > \dots > \theta_p}^{p-a_M} > 0 > \overbrace{\theta_{p+1} > \dots > \theta_{p+q-b_M}}^{q-b_M} > \overbrace{\theta_{p+q-b_M+1} > \dots > \theta_{p+q}}^{b_M} \quad (34)$$

WLOG, we can assume $\|\theta_1\| > \|\theta_{p+q}\|$ and define $g_M^{-1}(\theta_j) = \theta_j + s(M) \mathcal{R}_\mu(s(M)\theta_j^{-1})$. We will consider the limiting stable rank of the Hessians. From Proposition 3.2, the stable ranks of Hessians converges to the limiting stable ranks $\text{sr}\hat{\text{ank}}(H_N)$ and $\text{sr}\hat{\text{ank}}(H_M)$. Since $a_N > a_M$ and $b_N < b_M$, we can express the difference of the limiting stable rank of H_N and H_M as

$$\begin{aligned} &\text{sr}\hat{\text{ank}}(H_M) - \text{sr}\hat{\text{ank}}(H_N) \\ &= \sum_{j=2}^{a_M} \left\{ \left(\frac{g_M^{-1}(\theta_j)}{g_M^{-1}(\theta_1)} \right)^2 - \left(\frac{g_N^{-1}(\theta_j)}{g_N^{-1}(\theta_1)} \right)^2 \right\} + \sum_{j=a_M+1}^{a_N} \left\{ \left(\frac{U_M}{g_M^{-1}(\theta_1)} \right)^2 - \left(\frac{g_N^{-1}(\theta_j)}{g_N^{-1}(\theta_1)} \right)^2 \right\} + \\ &\quad \sum_{j=a_N+1}^{p+\alpha} \left\{ \left(\frac{U_M}{g_M^{-1}(\theta_1)} \right)^2 - \left(\frac{U_N}{g_N^{-1}(\theta_1)} \right)^2 \right\} + \sum_{j=1}^{b_M} \left\{ \left(\frac{g_M^{-1}(\theta_{p+q+1-j})}{g_M^{-1}(\theta_1)} \right)^2 - \left(\frac{g_N^{-1}(\theta_{p+q+1-j})}{g_N^{-1}(\theta_1)} \right)^2 \right\} + \\ &\quad \sum_{j=b_M+1}^{b_N} \left\{ \left(\frac{L_M}{g_M^{-1}(\theta_1)} \right)^2 - \left(\frac{g_N^{-1}(\theta_{p+q+1-j})}{g_N^{-1}(\theta_1)} \right)^2 \right\} + \sum_{j=b_N+1}^{q+\beta} \left\{ \left(\frac{L_M}{g_M^{-1}(\theta_1)} \right)^2 - \left(\frac{L_N}{g_N^{-1}(\theta_1)} \right)^2 \right\} \end{aligned} \quad (35)$$

We have six summation terms in (35) and will show each term is negative.

(i) Consider the first term in (35):

$$S_1 = \sum_{j=2}^{a_M} \left\{ \left(\frac{g_M^{-1}(\theta_j)}{g_M^{-1}(\theta_1)} \right)^2 - \left(\frac{g_N^{-1}(\theta_j)}{g_N^{-1}(\theta_1)} \right)^2 \right\}$$

We will show each term $F_j = \left(\frac{g_M^{-1}(\theta_j)}{g_M^{-1}(\theta_1)} \right)^2 - \left(\frac{g_N^{-1}(\theta_j)}{g_N^{-1}(\theta_1)} \right)^2$ in the summation is negative. We can expand F_j as follow:

$$\begin{aligned} F_j &= \left(\frac{g_M^{-1}(\theta_j)}{g_M^{-1}(\theta_1)} \right)^2 - \left(\frac{g_N^{-1}(\theta_j)}{g_N^{-1}(\theta_1)} \right)^2 \\ &= \left(\frac{g_M^{-1}(\theta_j)}{g_M^{-1}(\theta_1)} + \frac{g_N^{-1}(\theta_j)}{g_N^{-1}(\theta_1)} \right) \left(\frac{g_M^{-1}(\theta_j)}{g_M^{-1}(\theta_1)} - \frac{g_N^{-1}(\theta_j)}{g_N^{-1}(\theta_1)} \right) \\ &= \left(\frac{g_M^{-1}(\theta_j)}{g_M^{-1}(\theta_1)} + \frac{g_N^{-1}(\theta_j)}{g_N^{-1}(\theta_1)} \right) \left(\frac{g_M^{-1}(\theta_j)g_N^{-1}(\theta_1) - g_N^{-1}(\theta_j)g_M^{-1}(\theta_1)}{g_M^{-1}(\theta_1)g_N^{-1}(\theta_1)} \right) \end{aligned} \quad (36)$$

To verify the sign of F_j , we have to focus on the numerator of the second part of multiplicative term. We can simplify the numerator part as

$$\begin{aligned} &g_M^{-1}(\theta_j)g_N^{-1}(\theta_1) - g_N^{-1}(\theta_j)g_M^{-1}(\theta_1) \\ &= \theta_1 \{s(N)\mathcal{R}_\mu(s(N)\theta_j^{-1}) - s(M)\mathcal{R}_\mu(s(M)\theta_j^{-1})\} + \theta_j \{s(M)\mathcal{R}_\mu(s(M)\theta_1^{-1}) - s(N)\mathcal{R}_\mu(s(N)\theta_1^{-1})\} \\ &\quad + s(N)s(M) \{ \mathcal{R}_\mu(s(M)\theta_1^{-1})\mathcal{R}_\mu(s(N)\theta_j^{-1}) - \mathcal{R}_\mu(s(N)\theta_1^{-1})\mathcal{R}_\mu(s(M)\theta_j^{-1}) \} \end{aligned}$$

Consider the term:

$$F_{j,1} = \theta_1 \{s(N)\mathcal{R}_\mu(s(N)\theta_j^{-1}) - s(M)\mathcal{R}_\mu(s(M)\theta_j^{-1})\} + \theta_j \{s(M)\mathcal{R}_\mu(s(M)\theta_1^{-1}) - s(N)\mathcal{R}_\mu(s(N)\theta_1^{-1})\}$$

We know the R -transform can be expressed as power series as

$$\mathcal{R}_\mu(s(N)\theta^{-1}) = \sum_{n=1}^{\infty} C_n^{(\mu)} \left(\frac{s(N)}{\theta} \right)^{n-1}$$

where $C_n^{(\mu)}$ is the n -th cumulant of μ . Then we can calculate $F_{j,1}$ as

$$\begin{aligned} F_{j,1} &= \sum_{n=1}^{\infty} C_n^{(\mu)} (s(N)^n - s(M)^n) \theta_1 \cdot (1/\theta_j)^{n-1} - \sum_{n=1}^{\infty} C_n^{(\mu)} (s(N)^n - s(M)^n) \theta_j \cdot (1/\theta_1)^{n-1} \\ &= \sum_{n=1}^{\infty} C_n^{(\mu)} (s(N)^n - s(M)^n) \left(\theta_1 \cdot \left(\frac{1}{\theta_j} \right)^{n-1} - \theta_j \cdot \left(\frac{1}{\theta_1} \right)^{n-1} \right) \end{aligned}$$

Since $\theta_1 > \theta_j$ and $s(N) < s(M)$, we can easily show that $F_{j,1}$ is negative. Next, consider the term:

$$F_{j,2} = \mathcal{R}_\mu(s(N)\theta_j^{-1})\mathcal{R}_\mu(s(M)\theta_1^{-1}) - \mathcal{R}_\mu(s(M)\theta_j^{-1})\mathcal{R}_\mu(s(N)\theta_1^{-1})$$

By using the power series expression of \mathcal{R} -Transform, we have

$$F_{j,2} = \sum_{n=1}^{\infty} C_n^{(\mu)} \left(\frac{s(M)}{\theta_1} \right)^{n-1} \sum_{n=1}^{\infty} C_n^{(\mu)} \left(\frac{s(N)}{\theta_j} \right)^{n-1} - \sum_{n=1}^{\infty} C_n^{(\mu)} \left(\frac{s(N)}{\theta_1} \right)^{n-1} \sum_{n=1}^{\infty} C_n^{(\mu)} \left(\frac{s(M)}{\theta_j} \right)^{n-1}$$

We know that when $\sum_{n=1}^{\infty} a_n$ and $\sum_{n=1}^{\infty} b_n$ converges, then

$$\sum_1^{\infty} a_n \sum_1^{\infty} b_n = \sum_{n=1}^{\infty} \sum_{k=1}^n a_k b_{n-1+1}$$

Therefore, we have

$$\begin{aligned} F_{j,2} &= \sum_{n=1}^{\infty} \sum_{k=1}^n C_k^{(\mu)} C_{n-k+1}^{(\mu)} \left(\frac{s(N)}{\theta_j} \right)^{k-1} \left(\frac{s(M)}{\theta_1} \right)^{n-k} \\ &\quad - \sum_{n=1}^{\infty} \sum_{k=1}^n C_k^{(\mu)} C_{n-k+1}^{(\mu)} \left(\frac{s(M)}{\theta_j} \right)^{k-1} \left(\frac{s(N)}{\theta_1} \right)^{n-k} \\ &= \sum_{n=1}^{\infty} \sum_{k=1}^n C_k^{(\mu)} C_{n-k+1}^{(\mu)} \left\{ \left(\frac{s(N)}{\theta_j} \right)^{k-1} \left(\frac{s(M)}{\theta_1} \right)^{n-k} - \left(\frac{s(M)}{\theta_j} \right)^{k-1} \left(\frac{s(N)}{\theta_1} \right)^{n-k} \right\} \end{aligned}$$

If we let $T(n) = \sum_{k=1}^n C_k^{(\mu)} C_{n-k+1}^{(\mu)} \left\{ \left(\frac{s(N)}{\theta_j} \right)^{k-1} \left(\frac{s(M)}{\theta_1} \right)^{n-k} - \left(\frac{s(M)}{\theta_j} \right)^{k-1} \left(\frac{s(N)}{\theta_1} \right)^{n-k} \right\}$, we can write $F_{j,2} = \sum_{n=1}^{\infty} T(n)$. We will show $F_{j,2}$ is negative by showing each $T(n)$ is negative for $n = 2m$ and $n = 2m + 1$, where $m \in \mathbb{N}$. For $n = 2m$ ($m \in \mathbb{N}$),

$$\begin{aligned} T(n) &= T(2m) = \sum_{k=1}^{2m} C_k^{(\mu)} C_{2m-k+1}^{(\mu)} \left\{ \left(\frac{s(N)}{\theta_j} \right)^{k-1} \left(\frac{s(M)}{\theta_1} \right)^{2m-k} - \left(\frac{s(M)}{\theta_j} \right)^{k-1} \left(\frac{s(N)}{\theta_1} \right)^{2m-k} \right\} \\ &= \sum_{k=1}^m \left[C_k^{(\mu)} C_{2m-k+1}^{(\mu)} \left\{ \left(\frac{s(N)}{\theta_j} \right)^{k-1} \left(\frac{s(M)}{\theta_1} \right)^{2m-k} - \left(\frac{s(M)}{\theta_j} \right)^{k-1} \left(\frac{s(N)}{\theta_1} \right)^{2m-k} \right\} \right. \\ &\quad \left. - C_{2m-k+1}^{(\mu)} C_k^{(\mu)} \left\{ \left(\frac{s(N)}{\theta_j} \right)^{2m-k} \left(\frac{s(M)}{\theta_1} \right)^{k-1} - \left(\frac{s(M)}{\theta_j} \right)^{2m-k} \left(\frac{s(N)}{\theta_1} \right)^{k-1} \right\} \right] \\ &= \sum_{k=1}^m C_k^{(\mu)} C_{2m-k+1}^{(\mu)} (s(N)^{k-1} s(M)^{2m-k} - s(M)^{k-1} s(N)^{2m-k}) \left(\frac{1}{\theta_j^{k-1} \theta_1^{2m-k}} - \frac{1}{\theta_j^{2m-k} \theta_1^{k-1}} \right) \end{aligned}$$

We can easily show two conditions:

$$\begin{aligned} s(N)^{k-1} s(M)^{2m-k} - s(M)^{k-1} s(N)^{2m-k} &> 0 \iff 2m - 2k + 1 > 0 \\ \frac{1}{\theta_j^{k-1} \theta_1^{2m-k}} - \frac{1}{\theta_j^{2m-k} \theta_1^{k-1}} &> 0 \iff 2m - 2k + 1 < 0 \end{aligned}$$

Therefore, we can deduce $T(2m)$ is negative.

For $n = 2m + 1$ ($m \in \mathbb{N}$),

$$T(n) = T(2m + 1) = \sum_{k=1}^{2m+1} C_k^{(\mu)} C_{2m-k+2}^{(\mu)} \left\{ \left(\frac{s(N)}{\theta_j} \right)^{k-1} \left(\frac{s(M)}{\theta_1} \right)^{2m-k+1} - \left(\frac{s(M)}{\theta_j} \right)^{k-1} \left(\frac{s(N)}{\theta_1} \right)^{2m-k+1} \right\}$$

$(m + 1)$ -th term of $T(2m + 1)$ is zero since it is symmetric, thus we can write $T(2m + 1)$ as

$$T(2m+1) = \sum_{k=1}^m C_k^{(\mu)} C_{2m-k+2}^{(\mu)} (s(N)^{k-1} s(M)^{2m-k+1} - s(M)^{k-1} s(N)^{2m-k+1}) \left(\frac{1}{\theta_j^{k-1} \theta_1^{2m-k+1}} - \frac{1}{\theta_j^{2m-k+1} \theta_1^{k-1}} \right)$$

We can show $T(2m + 1)$ is negative as similar way of $T(2m)$. Therefore, F_j is negative.

(ii) Consider the second term in (35):

$$S_2 = \sum_{j=a_M+1}^{a_N} \left\{ \left(\frac{U_M}{g_M^{-1}(\theta_1)} \right)^2 - \left(\frac{g_N^{-1}(\theta_j)}{g_N^{-1}(\theta_1)} \right)^2 \right\}$$

We will show S_2 is negative by showing each term in the summation $G_j = \frac{U_M^2}{\{\theta_1 + s(M)\mathcal{R}_\mu(s(M)\theta_1^{-1})\}^2} - \left\{ \frac{\theta_j + s(N)\mathcal{R}_\mu(s(N)\theta_j^{-1})}{\theta_1 + s(N)\mathcal{R}_\mu(s(N)\theta_1^{-1})} \right\}^2$ is negative. Since $\theta_j + s(M)\mathcal{R}_\mu(s(M)\theta_j^{-1}) > U_M$ for all $j \in \{a_M + 1, \dots, a_N\}$, we have $G_j < F_j < 0$. Therefore, S_2 is negative.

(iii) Consider the third term in (35):

$$\begin{aligned} S_3 &= \sum_{j=a_N+1}^{p+\alpha} \left\{ \left(\frac{U_M}{g_M^{-1}(\theta_1)} \right)^2 - \left(\frac{U_N}{g_N^{-1}(\theta_1)} \right)^2 \right\} \\ &= (p + \alpha - a_N - 1) \left(\frac{U_M^2}{\{\theta_1 + s(M)\mathcal{R}_\mu(s(M)\theta_1^{-1})\}^2} - \frac{U_N^2}{\{\theta_1 + s(N)\mathcal{R}_\mu(s(N)\theta_1^{-1})\}^2} \right) \end{aligned}$$

By using the fact $U_N/s(N) = U_M/s(M)$, we can write the above term as

$$S_3 = (p + \alpha - a_N - 1) \left(\frac{U_M^2}{\{\theta_1 + s(M)\mathcal{R}_\mu(s(M)\theta_1^{-1})\}^2} - \frac{U_M^2}{\{\theta_1 + s(N)\mathcal{R}_\mu(s(N)\theta_1^{-1})\}^2} \frac{s(N)^2}{s(M)^2} \right)$$

By using the power series expansion of \mathcal{R} -Transform, we can easily show that $Q = 0$. For fourth, fifth, and sixth terms in (35), they are negative in similar way of (i), (ii), and (iii). Therefore, $\text{sr\`{a}nk}(H_M) - \text{sr\`{a}nk}(H_N)$ is negative. □

B Detail of the algorithms

B.1 Personalized Federated Low-Rank Updates (pFedLoRU)

Algorithm 2 pFedLoRU. \mathbf{W} is a model, $\mathbf{A}_0, \mathbf{B}_0$ are initial global low-rank update matrices, $\mathbf{L}_0, \mathbf{U}_0$ are initial personal low-rank update matrices, $\alpha_{\text{global}}, \alpha_{\text{per}}$ are the scaling factors, τ is an accumulation cycle, T is the total training round

Require: $\mathbf{W}, \mathbf{L}_0, \mathbf{U}_0, \mathbf{A}_0, \mathbf{B}_0, \alpha_{\text{global}}, \alpha_{\text{per}}, \tau, T$

Initialize: Server sends \mathbf{W} to each client, where client k initializes it as $\mathbf{W}^{(k)}$

for $t = 1, \dots, T$ **do**

Server selects M clients \mathcal{K}_M and distributes $\mathbf{A}_{t-1}, \mathbf{B}_{t-1}$

for each client $k \in \mathcal{K}_M$ **do**

Local training:

Find $\mathbf{L}_t^{(k)}, \mathbf{U}_t^{(k)}$ by solving (12) starting from $\mathbf{W}^{(k)} + \alpha_{\text{global}}\mathbf{A}_{t-1}\mathbf{B}_{t-1} + \alpha_{\text{per}}\mathbf{L}_{t-1}^{(k)}\mathbf{U}_{t-1}^{(k)}$

Find $\mathbf{A}_t^{(k)}, \mathbf{B}_t^{(k)}$ by solving (13) starting from $\mathbf{W}^{(k)} + \alpha_{\text{global}}\mathbf{A}_{t-1}\mathbf{B}_{t-1} + \alpha_{\text{per}}\mathbf{L}_t^{(k)}\mathbf{U}_t^{(k)}$

Send $\mathbf{A}_t^{(k)}, \mathbf{B}_t^{(k)}$ to the server.

end for

Server aggregation: $\mathbf{A}_t \leftarrow \sum_{k \in \mathcal{K}_M} p^{(k)} \mathbf{A}_t^{(k)}, \mathbf{B}_t \leftarrow \sum_{k \in \mathcal{K}_M} p^{(k)} \mathbf{B}_t^{(k)}$

if $t \bmod \tau = 0$ **then**

Server distributes $\mathbf{A}_t, \mathbf{B}_t$ to all clients

Each client k updates its local model: $\mathbf{W}^{(k)} \leftarrow \mathbf{W}^{(k)} + \alpha_{\text{global}}\mathbf{A}_t\mathbf{B}_t$

end if

end for

Return: $\mathbf{W}^{(k)} + \mathbf{L}_T^{(k)}\mathbf{U}_T^{(k)}$ for all client k

The pFedLoRU algorithm enables each client k to train a personalized model adapted to its data distribution. In pFedLoRU, client k retains global low-rank update matrices $\mathbf{A}^{(k)}$ and $\mathbf{B}^{(k)}$ for updating the shared model, as well as personalized low-rank update matrices $\mathbf{L}^{(k)}$ and $\mathbf{U}^{(k)}$ for learning the personalized model. The communication between the server and clients involves only the low-rank matrices \mathbf{A} and \mathbf{B} , which substantially reduces communication overhead. These matrices, \mathbf{A} and \mathbf{B} , are aggregated to update the global model $\mathbf{W}^{(k)}$. Finally, each client possesses a personalized model of the form $\mathbf{W}^{(k)} + \mathbf{L}^{(k)}\mathbf{U}^{(k)}$.

In practice, since the global model incorporates general knowledge from the all clients' dataset, and the personalized model is essentially a fine-tuned version of the global model, we typically assign higher ranks to $\mathbf{A}^{(k)}$ and $\mathbf{B}^{(k)}$. Additionally, although we use the same rank for $\mathbf{L}^{(k)}$ and $\mathbf{U}^{(k)}$ across all clients in our experiments, each client can, in practice, use different ranks based on the complexity and size of their local dataset. It is also noteworthy that different ranks for $\mathbf{A}^{(k)}$ and $\mathbf{B}^{(k)}$ can be employed by integrating pFedLoRU and mFedLoRU.

B.2 Model-Heterogeneous Federated Low-Rank Updates (mFedLoRU)

Algorithm 3 mFedLoRU. \mathbf{W} is a model, $\mathbf{A}_0, \mathbf{B}_0$ are initial low-rank update matrices, $\alpha, \alpha_A^{(k)}, \alpha_B^{(k)}$ are scaling factors, τ is an accumulation cycle, T is the total training round

Require: $\mathbf{W}, \mathbf{A}_0, \mathbf{B}_0, \alpha, \alpha_A^{(k)}, \alpha_B^{(k)}, \tau, T$
Initialize: Server sends \mathbf{W} to each client, where client k initializes it as $\mathbf{W}^{(k)}$
for $t = 1, \dots, T$ **do**
 Server selects M clients \mathcal{K}_M and distributes $\mathbf{A}_{t-1}, \mathbf{B}_{t-1}$
 for each client $k \in \mathcal{K}_M$ **do**
 Initializes nested low-rank updates $\mathbf{A}_{d,t-1}^{(k)}, \mathbf{A}_{u,t-1}^{(k)}$ and $\mathbf{B}_{d,t-1}^{(k)}, \mathbf{B}_{u,t-1}^{(k)}$
 Local training:
 Find $\mathbf{A}_{d,t}^{(k)}, \mathbf{A}_{u,t}^{(k)}, \mathbf{B}_{d,t}^{(k)}, \mathbf{B}_{u,t}^{(k)}$ by solving (15)
 starting from $\mathbf{W}^{(k)} + \alpha(\mathbf{A}_{t-1} + \alpha_A^{(k)} \mathbf{A}_{d,t-1}^{(k)} \mathbf{A}_{u,t-1}^{(k)})(\mathbf{B}_{t-1} + \alpha_B^{(k)} \mathbf{B}_{d,t-1}^{(k)} \mathbf{B}_{u,t-1}^{(k)})$
 Sends $\mathbf{A}_{d,t}^{(k)} \mathbf{A}_{u,t}^{(k)}$ and $\mathbf{B}_{d,t}^{(k)} \mathbf{B}_{u,t}^{(k)}$ to the server
 end for
 Recover rank- r low-rank updates from hierarchical low-rank updates:
 $\mathbf{A}_t^{(k)} \leftarrow \mathbf{A}_{t-1} + \alpha_A^{(k)} \mathbf{A}_{d,t}^{(k)} \mathbf{A}_{u,t}^{(k)}, \mathbf{B}_t^{(k)} \leftarrow \mathbf{B}_{t-1} + \alpha_B^{(k)} \mathbf{B}_{d,t}^{(k)} \mathbf{B}_{u,t}^{(k)}$
 Server aggregation: $\mathbf{A}_t \leftarrow \sum_{k \in \mathcal{K}_M} p^{(k)} \mathbf{A}_t^{(k)}, \mathbf{B}_t \leftarrow \sum_{k \in \mathcal{K}_M} p^{(k)} \mathbf{B}_t^{(k)}$
 if $t \bmod \tau = 0$ **then**
 Server distributes $\mathbf{A}_t, \mathbf{B}_t$ to all clients
 Each client k updates its local model: $\mathbf{W}^{(k)} \leftarrow \mathbf{W}^{(k)} + \alpha \mathbf{A}_t \mathbf{B}_t$
 end if
 end for
Return: $\mathbf{W} + \sum_{t=1: t \bmod \tau=0}^T \mathbf{A}_t \mathbf{B}_t$

The mFedLoRU algorithm enables each client k to utilize a rank tailored to its resource constraints. Similar to FedLoRU, client k maintains low-rank update matrices $\mathbf{A}^{(k)} \in \mathbb{R}^{m \times r}$ and $\mathbf{B}^{(k)} \in \mathbb{R}^{r \times n}$, but employs recursive low-rank updates during training. First, client k determines personal update ranks $r_A^{(k)}, r_B^{(k)} < r$ based on its resources. At each round, it initializes nested low-rank update matrices $\mathbf{A}_d^{(k)} \in \mathbb{R}^{m \times r_A^{(k)}}$, $\mathbf{A}_u^{(k)} \in \mathbb{R}^{r_A^{(k)} \times r}$ and $\mathbf{B}_d^{(k)} \in \mathbb{R}^{r \times r_B^{(k)}}$, $\mathbf{B}_u^{(k)} \in \mathbb{R}^{r_B^{(k)} \times n}$ such that $\mathbf{A}_d^{(k)} \mathbf{A}_u^{(k)} = 0$ and $\mathbf{B}_d^{(k)} \mathbf{B}_u^{(k)} = 0$. After local training by solving (15), we can update client k 's original low-rank matrices as follows:

$$\mathbf{A}^{(k)} \leftarrow \mathbf{A}^{(k)} + \alpha_A^{(k)} \mathbf{A}_d^{(k)} \mathbf{A}_u^{(k)}, \quad \mathbf{B}^{(k)} \leftarrow \mathbf{B}^{(k)} + \alpha_B^{(k)} \mathbf{B}_d^{(k)} \mathbf{B}_u^{(k)} \quad (37)$$

In mFedLoRU, to reduce communication overhead, the client does not recover its original low-rank matrices directly. Instead, it sends the nested low-rank matrices to the server, and the server recovers them. By using this strategy, the communication overhead is reduced from $2mn$ to $r(m+n) + r_A(m+r) + r_B(n+r)$.

B.3 Personalized Federated Low-Rank Adaptation (pFedLoRA)

We outline two variants of the personalized FedLoRA algorithm here. Both versions of pFedLoRA follow a similar framework, where each client maintains a full-rank global model \mathbf{W} and its own personalization modules $\mathbf{L}^{(k)}$ and $\mathbf{U}^{(k)}$.

In pFedLoRA(1), the first variant, as suggested by Wu et al. (2024) and other FedLoRA algorithms, the personalization modules are optimized separately from the global model. Specifically, the algorithm first optimizes the personalization modules for E_{per} and subsequently optimizes the global full-rank model for E_{global} by solving:

$$\mathbf{L}_t^{(k)}, \mathbf{U}_t^{(k)} = \arg \min_{\mathbf{L}, \mathbf{U}} f^{(k)}(\mathbf{W}^{(k)} + \alpha_{\text{per}} \mathbf{L} \mathbf{U}) \quad (38)$$

$$\mathbf{W}_t^{(k)} = \arg \min_{\mathbf{W}} f^{(k)}(\mathbf{W} + \alpha_{\text{per}} \mathbf{L}_t^{(k)} \mathbf{U}_t^{(k)}) \quad (39)$$

Algorithm 4 pFedLoRA. \mathbf{W} is a model, $\mathbf{L}_0, \mathbf{U}_0$ are initial personal low-rank update matrices, α_{per} is the scaling factor, T is the total training round.

Require: $\mathbf{W}, \mathbf{L}_0, \mathbf{U}_0, \alpha_{\text{per}}, T$.

Initialize: Server sends \mathbf{W} to each client, where client k initializes it as $\mathbf{W}^{(k)}$.

for $t = 1, \dots, T$ **do**

Server selects M clients \mathcal{K}_M and distributes \mathbf{W}_{t-1} and client k initializes it as $\mathbf{W}^{(k)}$.

for each client $k \in \mathcal{K}_M$ **do**

Local training - pFedLoRA(1):

Find $\mathbf{L}_t^{(k)}, \mathbf{U}_t^{(k)}$ by solving (38) starting from $\mathbf{W}^{(k)} + \alpha_{\text{per}} \mathbf{L}_{t-1}^{(k)} \mathbf{U}_{t-1}^{(k)}$

Find $\mathbf{W}_t^{(k)}$ by solving (39) starting from $\mathbf{W}^{(k)} + \alpha_{\text{per}} \mathbf{L}_t^{(k)} \mathbf{U}_t^{(k)}$

Local training - pFedLoRA(2):

Find $\mathbf{W}_t^{(k)}, \mathbf{L}_t^{(k)}, \mathbf{U}_t^{(k)}$ together by solving (40) starting from $\mathbf{W}^{(k)} + \alpha_{\text{per}} \mathbf{L}_{t-1}^{(k)} \mathbf{U}_{t-1}^{(k)}$

Send $\mathbf{W}_t^{(k)}$ to the server.

end for

Server aggregation: $\mathbf{W}_t \leftarrow \sum_{k \in \mathcal{K}_M} p^{(k)} \mathbf{W}_t^{(k)}$

end for

Return: $\mathbf{W}_T + \mathbf{L}_T^{(k)} \mathbf{U}_T^{(k)}$ for all client k

However, pFedLoRA(1) has been found to be less effective compared to our modified version pFedLoRA(2). The second variant, pFedLoRA(2), optimizes both the personalization modules and the global full-rank model simultaneously for $E = E_{\text{per}} + E_{\text{global}}$ by solving:

$$\mathbf{W}_t^{(k)}, \mathbf{L}_t^{(k)}, \mathbf{U}_t^{(k)} = \arg \min_{\mathbf{W}, \mathbf{L}, \mathbf{U}} f^{(k)}(\mathbf{W} + \alpha_{\text{per}} \mathbf{L} \mathbf{U}) \quad (40)$$

C Detail of the experiment setting

In this section, we provide a detailed explanation of the experiments, including the datasets and hyperparameters used. The implementation is based on PyTorch.

C.1 Detail of the implementation in experiments

Detailed implementation of FedLoRU In FedLoRU, FedHM, and their variant algorithms, we generate factorized low-rank modules for convolutional layers only. We utilize several low-rank environments where the rank of the factorized low-rank modules are 16, 32, 64, 128. Further, we use $\alpha = 16$ for all experiments as it turns out to have consistent results for $\alpha \in \{16, 32, 64\}$.

Federated learning setting The federated learning experiments were conducted using three datasets: CIFAR-10, CIFAR-100, and Alpaca. The client sampling rate, representing the proportion of clients selected per communication round, was set at 0.5 for all datasets. Each client performed 5 local epochs per communication round on CIFAR-10 and CIFAR-100 with a batch size of 32, while client performed 1 local epochs on Alpaca with a batch size of 16. The optimizer used for training was stochastic gradient descent (SGD) with a momentum of 0.9 on CIFAR-10 and CIFAR-100, while AdamW (Loshchilov, 2017). We find the learning rate using grid search and use Cosine-Annealing as scheduler, and the cycle step is set to 50 or the total communication round.

Model heterogeneous setting In this subsection, we describe the system heterogeneous settings used in our experiments. To simulate varying client capabilities, we tested two different system heterogeneous configurations in mFedLoRU experiments where the clients had different ranks, denoted as r , which reflect the computational resources or constraints of each client. For FedHM, we match the number of trainable parameters corresponding to the model with specific rank in mFedLoRU experiments.

Rank of a client		$r = 128$	$r = 64$	$r = 32$	$r = 16$
#Clients	setting 1	5	5	5	5
	setting 2	-	6	6	7

Table A1: Detailed system heterogeneous settings in our experiments. Both settings include total 20 clients.

The motivation behind these settings was to create a challenging system heterogeneous environment. This is particularly important since we observed that FedLoRU with $r = 128$ produces similar results to FedAvg with a full-rank model. Hence, these settings were designed to push the algorithm’s adaptability under harsher, more diverse client conditions.